Effect of molecular structure on autoignition temperature of hydrocarbon fuels

Colin Gray

Final Report: September 27, 2024

Mentors: Charline Fouchier and Professor Joseph E. Shepherd

Explosion Dynamics Laboratory, California Institute of Technology, Pasadena, CA

Abstract

The autoignition temperature or AIT is the minimum temperature at which a fuel ignites in a vessel of hot air, causing combustion without an external ignition source. The AIT of a fuel is one way of evaluating the risk of accidental combustion hazards in hot environments. However, the exact relationship of fuel composition to AIT is not well understood, and further investigation is required to enable the synthesis of fuels with desired properties. The ASTM-E659 test is the industry standard for measuring AIT and the previous projects in Prof. Shepherd's laboratory have created an automated injection apparatus to increase repeatability. Using this apparatus, we measured the AIT of different fuel compositions with distinct characteristics and studied the correlation between specific structures and the subsequent AIT. For example, investigation into aromatic content has shown higher aromatic content results in higher AIT. The relationship between compactness/branching of fuel components and AIT is also investigated. Results from this project may lead to a better understanding of AIT and provide guidance for future development of synthetic fuels for the aviation industry.

Contents

1 Introduction 3

1.1 Background and motivation 3

1.1.1 Methods of autoignition experimentation and existing results 3

1.1.2 The chemistry of low-temperature autoignition 4

1.1.3 Modes of ignition 5

1.1.4 Initial investigation and planning 9

1.2 Research plan 10

2 Methods 11

2.1 Data acquisition 11

2.2 Materials 12

3 Results 13

3.1 Visualization of results 13

3.2 Aromatic content results 13

3.2.1 Summary of aromatic content results 13

3.2.2 Individual aromatic content fuel graphs 14

3.2.3 Activation energies 17

3.3 Branching results 18

3.3.1 Summary of branching results 18

3.3.2 Individual branching fuel graphs 19

4 Discussion 22

4.1 Modes of ignition 22

4.2 Aromatic content 23

4.3 Branching 23

5 Conclusions and future work 24

6 Acknowledgements 24

7 References 25

8 Supplemental materials 25

1 Introduction

1.1 Background and motivation

1.1.1 Methods of autoignition experimentation and existing results

The autoignition temperature (AIT) is the minimum temperature at which a material self-ignites, causing combustion without an external ignition source. Low-temperature, less than 500°C, autoignition of hydrocarbon fuels is of particular interest for minimizing fire and explosion hazards in the manufacturing, distribution, and end-use of commodity fuels in the transportation and aviation industries. The industry standard used in the USA to determine AIT is ASTM-E659 [1]. The standard uses an apparatus consisting of a heated glass flask filled with hot air (Figure 1) into which fuel is injected using a prescribed procedure to find the minimum temperature at which self-ignition occurs. The Explosion Dynamics Lab (EDL) at Caltech has utilized the ASTM-E659 apparatus to study low-temperature autoignition of various commercial fuels such as aviation kerosene (Jet A), synthetic paraffinic kerosene, fuel surrogates, and pure substances. Previous projects in the lab have worked to automate the injection and measurement process to remove the effects of human error on injection speed, angle, volume, etc. The experimentation done during this project demonstrates repeatable and consistent results when testing one fuel at the same temperature multiple times (Figure 2).

The most important factor that determines the AIT of a fuel at atmospheric pressure is the chemical composition. Thus, understanding the relationship between the structure of fuel components and the subsequent AIT would guide the synthesis of fuels with desired characteristics. Synthetic fuels derived from sustainable resources are of interest to the aviation industry to reduce the environmental impact of aviation kerosene produced from petroleum. Previous research has been published regarding the correlation between hydrocarbon structure and the AIT of pure components by Affens et al. [2] who investigated the AIT of pure compounds with a precursor apparatus to the ASTM-E659 test.

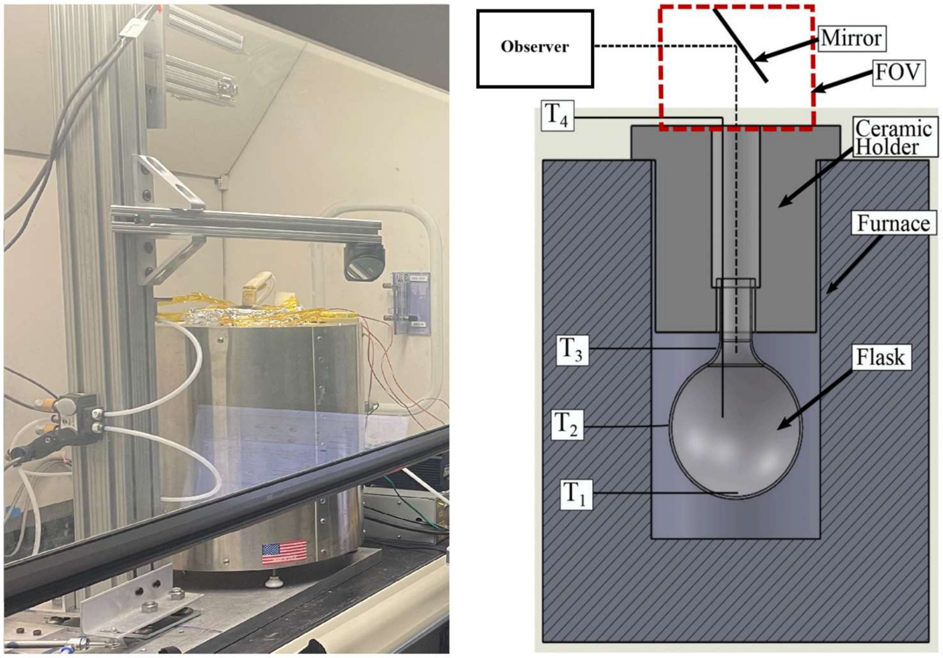

(a) (b)

Figure 1: a) Picture of ASTM-E659 testing apparatus. b) cross-sectional schematic of ASTM-E659 test apparatus [3].

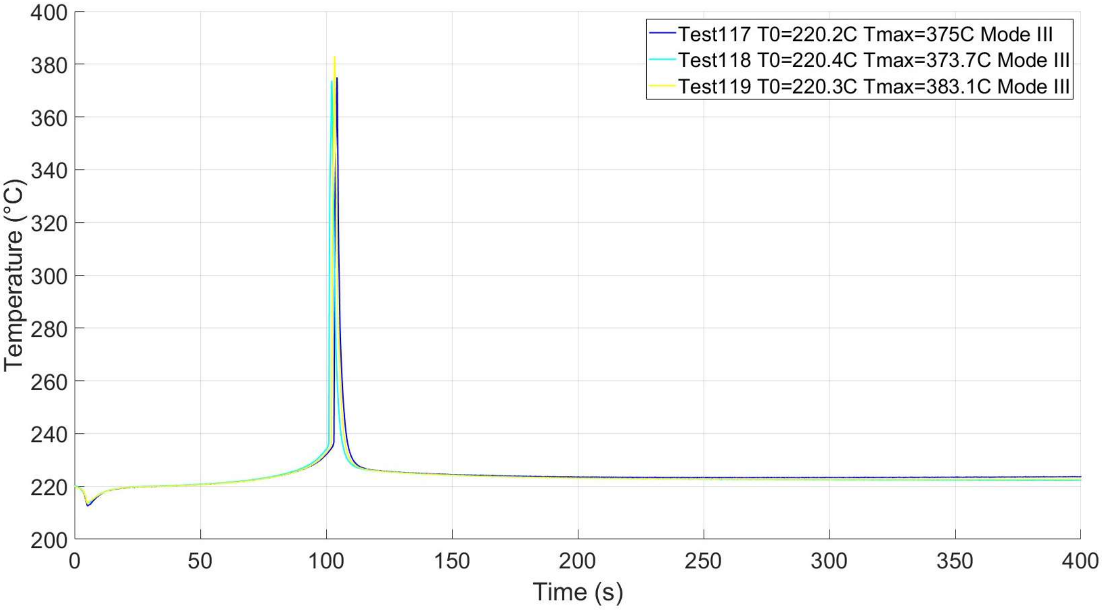

Figure 2: The signal from the T4 probe of the ASTM-E659 apparatus. All three tests are of a component fuel consisting of 20% 2,2,4-trimethylbenzene and 80% 2-methyloctane by weight. These tests were run at nearly identical initial temperatures and demonstrate the consistency of the EDL's automated ASTM-E659 injection system.

Some correlations found include increased AIT as the chain length, number of methyl groups, and unsaturated bonds decreased. Affens et al. [2] also noted a higher AIT for aromatic molecules as compared to normal cyclic molecules. However, due to the complexity and multitude of reactions that occur during combustion, the role of hydrocarbon structure on the AIT in non-pure fuels is not well understood. A goal of our investigation is to examine some simple fuel blends, measure the AIT and compare with the correlations reported in the literature and chemical databases.

1.1.2 The chemistry of low-temperature autoignition

One key distinction between the low-temperature autoignition (600 - 850K) investigated in this study and high-temperature autoignition (1000K or greater) is the complexity of the chemical reactions. Combustion generally begins with hydrogen abstraction which creates highly reactive radical intermediates, and the reactions propagate in a rapid chain reaction that terminates with the exothermic reactions to create the main products, water and carbon dioxide [4]. Reaction 3 in Figure 3 demonstrates a simplified pathway for high-temperature autoignition, with notably less intermediates than other pathways. At temperatures above 1000K, molecular decomposition favors the direct formation of alkyl radicals and a 1-alkene molecule. This fast and direct decomposition of fuel molecules with few intermediates compared to other pathways, as well as quicker hydrogen abstraction due to higher available energy, leads to a faster reaction with fewer intermediates [4].

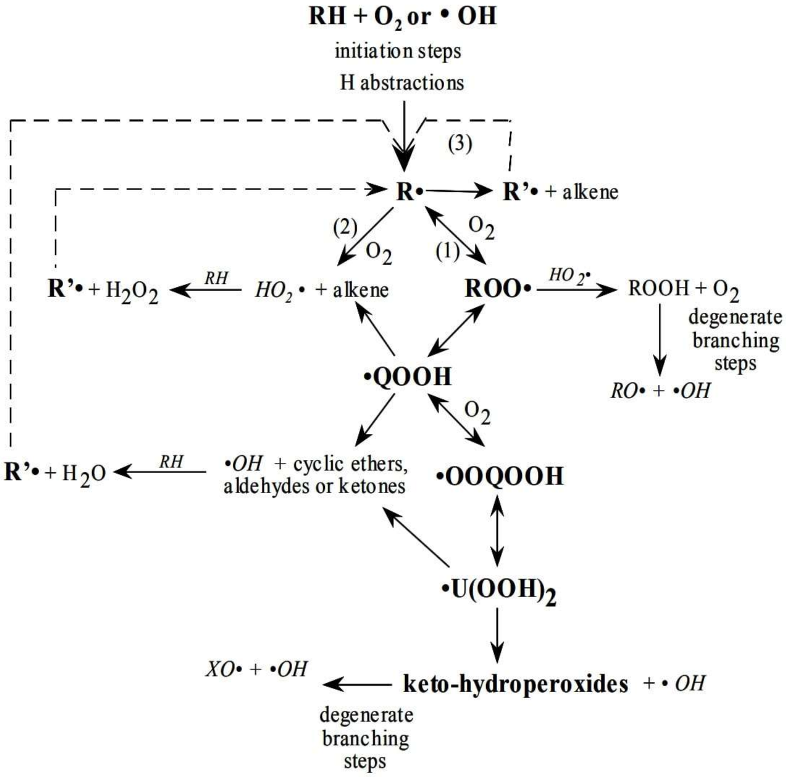

Figure 3: Simplified scheme for the primary mechanism of oxidation of alkanes from [4].

Low-temperature autoignition, occurring generally between 600 and 850K, is characterized by a more complex network of chemical reactions involving reactive intermediates. Unlike high-temperature ignition with quick and direct reactions that break apart fuel molecules, low-temperature pathways begin with formation of peroxy radicals (ROO•) after hydrogen abstraction [4]. As demonstrated by Reaction 1 and subsequent pathways on Figure 3, these radicals can react with oxygen to form hydroperoxides (ROOH) and lead to degenerate branching, creating more radicals which contribute to additional reaction pathways. The peroxy radicals can also undergo isomerization steps, leading to hydroperoxyalkyl radicals (•QOOH), the reactants for subsequent bottom pathways shown on Figure 3. The presence of these intermediates makes low-temperature autoignition much more complex than its high-temperature counterpart. The reactions can take many forms, including the formation of cyclic ethers, aldehydes, or even partial oxidation products like ketones [4]. This slower progression, alongside lower energy release, can result in phenomena like cool flames, where partial combustion occurs with minimal heat and light production. The numerous reaction pathways make low-temperature autoignition intricate to model. As a result – compared to high-temperature autoignition– low-temperature autoignition is particularly not well understood, and test data will require further experimentation and modeling to fully decipher.

1.1.3 Modes of ignition

Previous autoignition experimentation at EDL had classified four types of ignitions [3], ranging from Mode I to Mode IV as shown in the table below (Table 1). As discussed in [5], no ignition (also called Mode 0 in this report) and Mode IV are both considered as non-ignition cases with temperature rises or "spikes" of less than 15°C or greater than 15°C but still small temperature spikes compared to the other modes, respectively. Mode III and Mode I are both ignition cases with substantial temperature spikes (>>15°C). However, Mode I has a large luminous flame visible to the naked eye, whereas Mode III does not. Mode II was not observed in the initial experimentation; however Mode II is difficult to distinguish without a sensitive camera or photodiode, which was not used in this investigation. This original classification may have its limits and may not be suitable for all fuels, see the Discussion for further comments.

Ignition Mode	Name	Luminosity	Temperature Rise (ΔT)
I	Ignition	Large	Large
II	Cool Flame	Small	Small
III	Non-Luminous Cool Flame	None	Large
IV	Rapid Reaction	None	Small
-	Non-ignition	None	<15°C

Table 1: Classifications of various ignition modes observed in ASTM-E659 [3]. In all figures below, the "Non-ignition" case is labeled as "Mode 0."

An important difference between the study [3] used for the above classification and the present experiments is that careful observation in a completely dark room was used in [3]. The present tests were done in ambient lighting with dimmed lights, and with only the human eye and regular camera, thus Mode II cannot be confidently identified. Mode IV ignition, a type of non-ignition, occurs when there is a small but visible temperature rise (i.e., a slow exothermic reaction) as shown in Figure 4. Mode III ignition shows a significant temperature spike (i.e., a rapid exothermic reaction) and either a puff of smoke or a lack of phenomena visible to the human eye as compared to Mode I ignition (Figures 5 and 6). Mode I ignition shows a bright flash of visible flame (Figures 7 and 8). The examples of these cases shown in Figs. 4-8 are for “30% TMB” tests described in Methods.

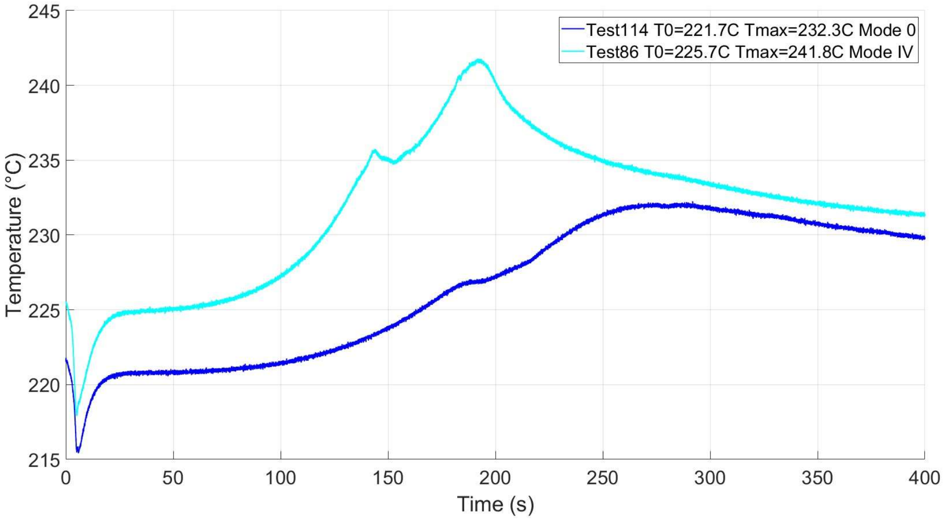

Figure 4: Mode 0 (no ignition) and Mode IV ignition of 30% TMB. Mode 0 simply indicates no ignition or substantial chemical reaction. As shown, the Mode IV case has a more substantial temperature increase, ~16°C, which puts it outside the range of no-ignition or Mode 0.

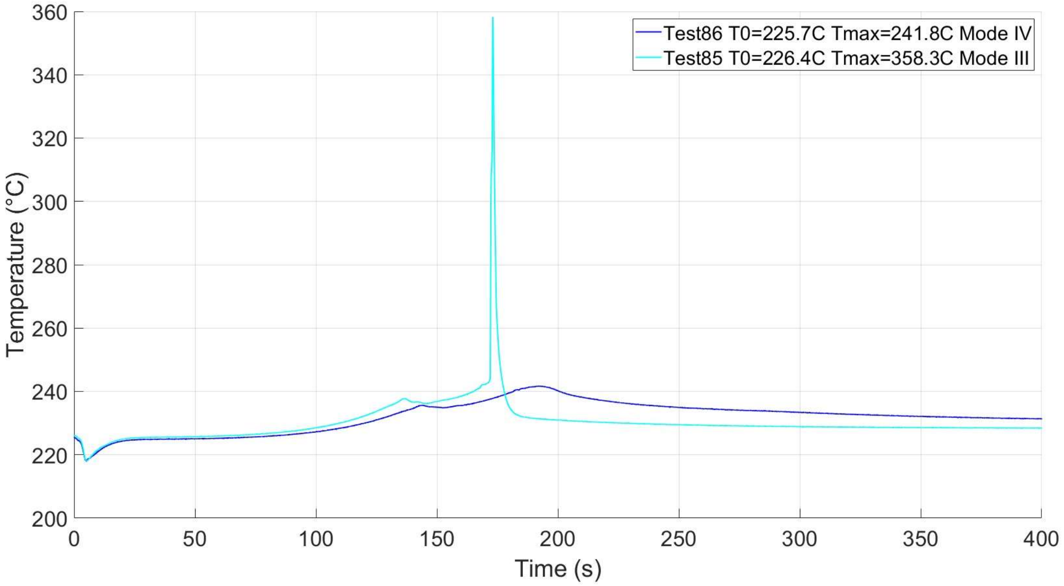

Figure 5: Mode IV and Mode III ignition of 30% TMB. Despite an initial temperature difference of only 0.7 ± 2.2°C, Test 85 (Mode III) has a maximum temperature 116.5 ± 2.2°C, higher than Test 86 (Mode IV), showing the difference between the Mode IV rapid reaction non-ignition case and the Mode III ignition case.

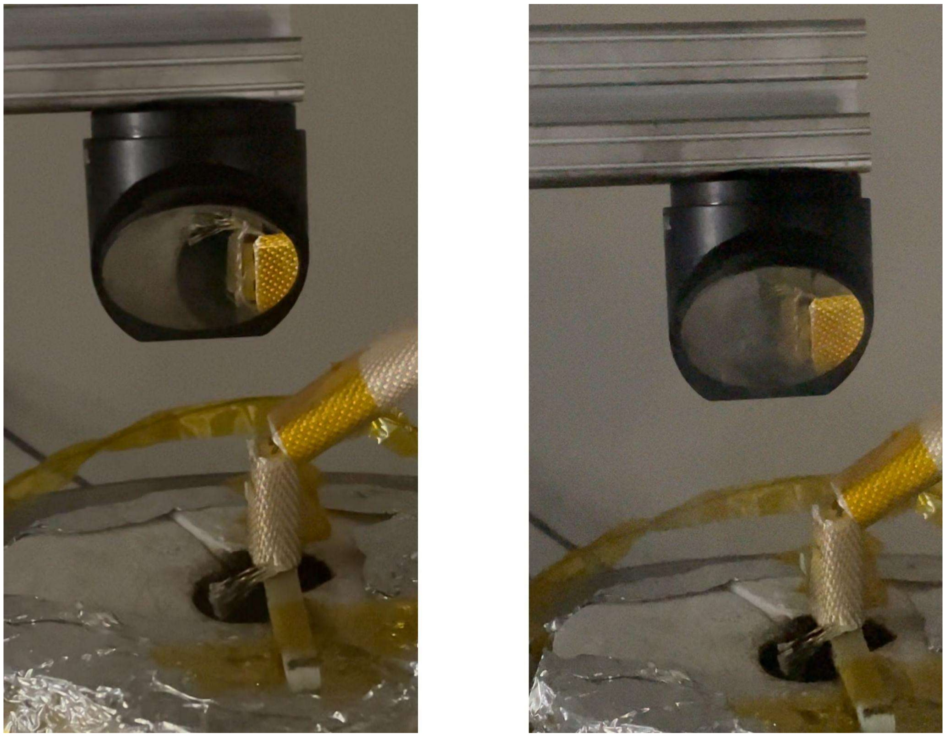

Figure 6: Mode III ignition. The left image shows right before ignition compared to the right image which from during/after Mode III ignition. The entrance to the flask becomes obscured from the puff of vapors due to ignition.

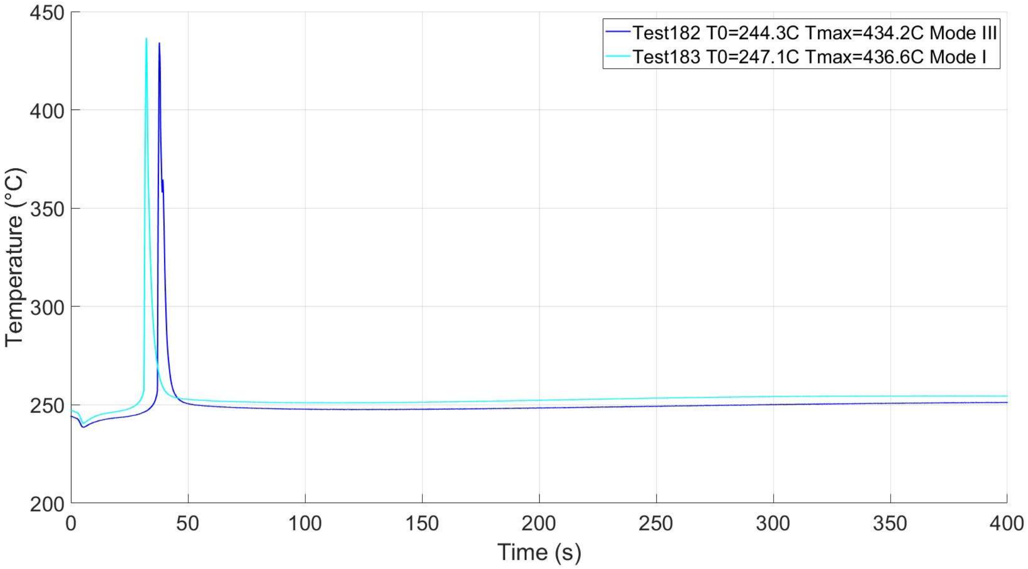

Figure 7: Mode III and Mode I ignition of 30% TMB. Graphically, there is often very little difference that can be observed, as shown above, other than a higher maximum temperature and earlier ignition time for Mode I. However, there is a clear visible difference as shown by comparing Figure 6 to Figure 8.

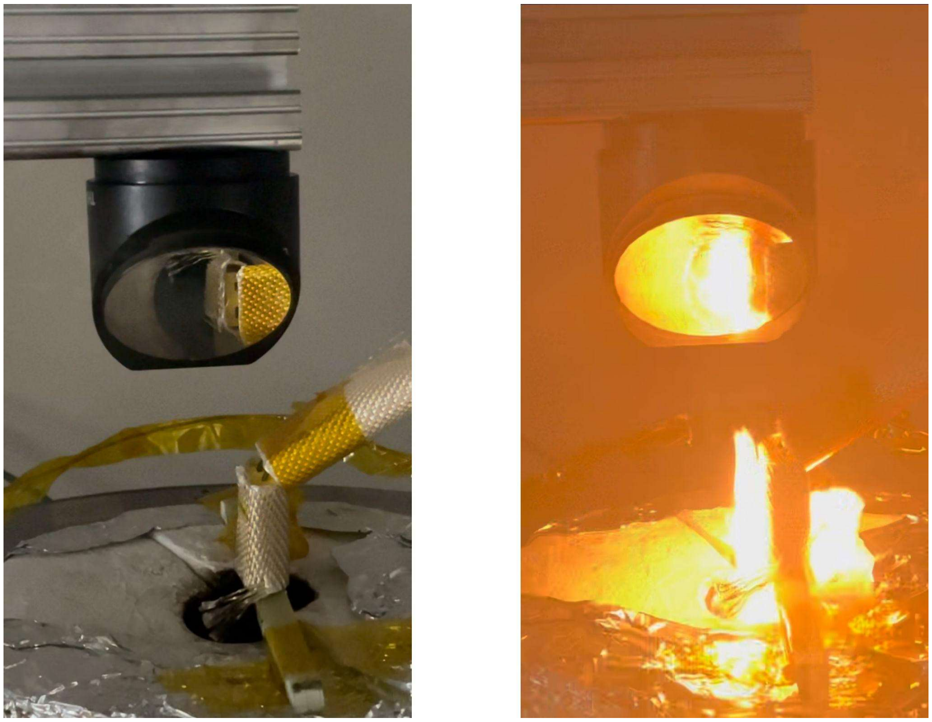

Figure 8: Mode I ignition. The left image is before Mode I ignition, and the right image is during Mode I ignition.

1.1.4 Initial investigation and planning

Recently, the EDL has been investigating the ignition properties of an alternative to Jet A, a synthetic paraffinic kerosene (SPK). This particular SPK has been found to have a lower AIT than Jet A. By performing mass spectrometry on a sample of Jet A and SPK, it was found that SPK was missing several of the components in Jet A, especially aromatic molecules [5]. In addition, the Affens et al. [2] study found that aromatic compounds tend to have higher AIT than non-aromatic compounds. Thus, the effect of aromaticity in a multiple-component fuel was one subject of interest in this investigation.

By combining AIT information from the DIPPR database [6], the paper by Affens et al. [2], and from the Chemical Properties Handbook by Carl L. Yaws [7], an analysis was conducted to explore possible correlations between structural characteristics and reported AIT. For the full dataset, see the supplemental Preliminary Investigation Excel file and additional graphical material in Appendix B. Among molecules with the same number of carbons, having a double bond will increase AIT, as well as having one methyl group vs. an entirely straight carbon chain (Figure 9). For example, an eight-carbon straight chain with no double bonds will have lower AIT than an eight-carbon straight chain with one double bond. In addition, eight carbons in a straight chain will have a lower AIT than seven carbons in a straight chain with the eighth carbon in a methyl group. This suggested that having more methyl groups would raise AIT vs. having the carbons in a straight chain. Figure 10 provides more evidence of this, showing that with a nine-carbon molecule, the reported AIT increases with the number of methyl groups (Figure 10). Thus, our second topic of investigation is to find if this correlation exists for a multi-component fuel, possibly indicating that branching could be used as one parameter to control the AIT of a fuel.

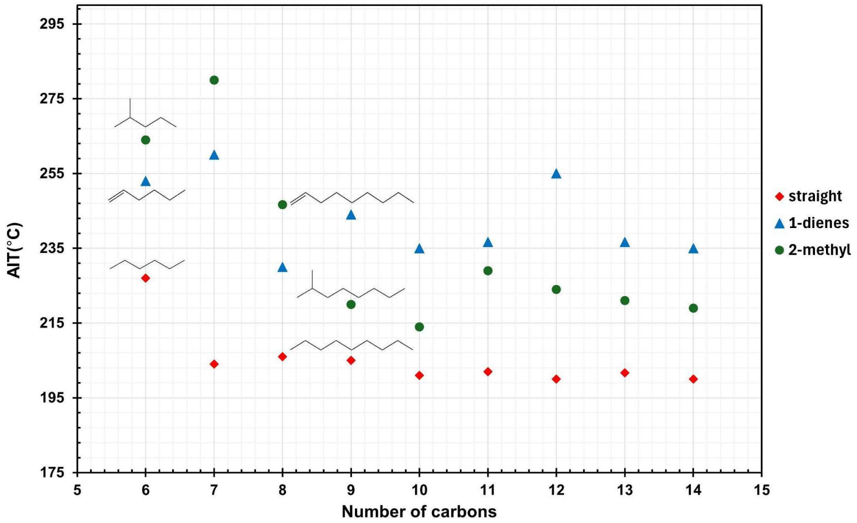

Figure 9: Reported AIT versus the number of carbons within molecules of different groups. 1-dienes refer to molecules with a double bond between the first and second carbon. 2-methyl refers to molecules with a methyl group on the second carbon. Representative molecular structures are shown for the six-carbon and nine-carbon groups.

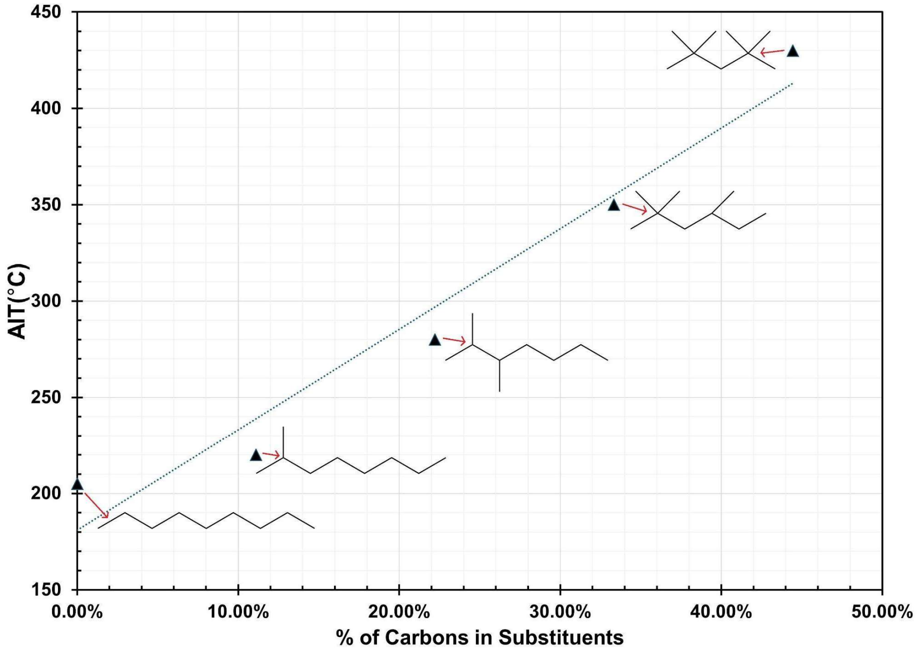

Figure 10: Reported AIT vs the % of carbons that are in methyl groups within nine-carbon hydrocarbons. This graph shows the correlation between the presence of a methyl group and the AIT with the addition of methyl groups, thus providing a clear second target of investigation. The molecular structure corresponding to each data point is shown on the graph.

1.2 Research plan

Previous work [3] performed in the EDL investigated two surrogate fuels that resembled Jet A's ignition characteristics, one of which was the Aachen surrogate [8]. This surrogate fuel was 80 wt% n-decane and 20 wt% 1,2,4-trimethylbenzene (TMB) (Table 2), and "exhibited similar ignition behavior to Jet A with comparable AITs," [3]. To investigate both branching and aromatic content the present study used a similar two-component fuel with n-nonane and TMB. The decision to use these components comes from availability of these chemicals in the EDL from the previous work and the simplicity of the surrogate fuel. N-nonane was chosen over n-decane because the higher branched isomers of n-nonane required to investigate branching were more readily and cheaply available in necessary volumes than the isomers of n-decane. Both n-decane and n-nonane are straight chain molecules, and according to the DIPPR database, have similar AITs, only differing by 4°C. To test branching, the chosen isomers of n-nonane are 2-methyloctane, 2,2,4-trimethylhexane, and 2,2,4,4-tetramethylpentane (Table 2); 2,3-dimethylheptane was not investigated due to high cost.

Name	Structure	# of Carbons	Reported AIT (°C)	# of Methyl Groups
1,2,4-trimethylbenzene		9	515	3
n-nonane		9	205	0
2-methyloctane	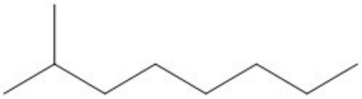	9	220	1
2,2,4-trimethylhexane	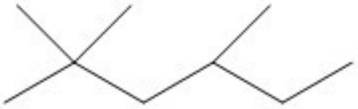	9	350*	3
2,2,4,4-tetramethylpentane		9	430*	4

*'Predicted' values from the DIPPR database, have an uncertainty of ">25%".

Table 2: Reported autoignition temperature and relevant structural characteristics of the hydrocarbons used in this study. All AITs come from the DIPPR database, and the primary data sources are not cited. However, the AITs are useful for guiding the direction of research.

2 Methods

2.1 Data acquisition

All testing was completed using the automated ASTM-E659 apparatus (Figure 1). Each test was run with 300 µL of component fuels. The furnace controlling the temperature of the ASTM-E659 was turned on several hours before the first test to allow thermal stabilization. Before the first test, and between each test, the stability of the furnace temperature was checked by monitoring a live feed of the T4 thermocouple to ensure the air temperature inside the flask was not increasing or decreasing. Each test was taken with a 30-second initial condition period at 75 Hz, the average of which is the initial temperature of each test, or "T0". After the 30-second initial condition temperature acquisition period, the 300 µL injection occurred over 3-4 seconds. The acquisition of the temperature from T4 started simultaneously alongside the injection and was recorded at 75 Hz for 400 seconds. Once the 400-second data acquisition period ended, the flask was flushed using a heat gun, the furnace was changed to the next temperature for testing, and the flask was given around an hour to stabilize. Once stabilized, the next test would be run. The furnace would be cleaned every couple of days by raising the temperature to 550°C to vaporize any byproducts deposited on the flask.

2.2 Materials

To investigate the correlation between aromatic content and AIT, four component fuels were synthesized according to Table 3. The volumes shown were measured using a volumetric pipette, were added to a bottle and shaken vigorously to mix and double-checked visually to confirm no separation of fuel components. 50 mL was made of each n-nonane fuel. Fuels were named based on the aromatic content.

Fuel Name	Component 1 (by wt.)	Component 2 (by wt.)
0% TMB	100% n-nonane (50 mL)	0% TMB
10% TMB	90% n-nonane (45.8 mL)	10% TMB (4.2 mL)
20% TMB	80% n-nonane (41.5 mL)	20% TMB (8.5 mL)
30% TMB	70% n-nonane (37.0 mL)	30% TMB (13.0 mL)

Table 3: Component fuels for aromatic content testing.

To investigate the correlation between branching and AIT, the '20% TMB' fuel from the aromatic content experimentation was used together with 3 new two-component fuels that differ based on component 1 (Table 4). As the goal is to find how the increase of branching affects AIT, all four component fuels are 20 wt% TMB, and 80 wt% of the molecule of interest, as shown below. Besides the previously formulated 20% TMB fuel, the fuels were synthesized using a 100-1000 μL micropipette, as only 5 mL of each nonane isomer was ordered. Thus, 5 mL of each component fuel was made, limiting the number of possible tests. Fuels were named based on the nonane isomer.

Fuel Name	# of Methyl Groups	Component 1	Component 2
"20% TMB" (n-nonane)	0	n-nonane (41.5 mL)	TMB (8.5 mL)
2-methyloctane	1	2-methyloctane (4160 μL)	TMB (840 μL)
2,2,4-trimethylhexane	3	2,2,4-trimethylhexane (4155 μL)	TMB (845 μL)
2,2,4,4-tetramethylpentane	4	2,2,4,4-tetramethylpentane (4152 μL)	TMB (848 μL)

Table 4: Two-component fuels for branching testing. Each two-component fuel was 80% by weight of component 1 and 20% by weight of component 2. Refer to Table 2 for '# of Methyl Groups'.

The percent uncertainty of each aromatic content fuel was calculated using a 0.03 mL error of the 25 mL graduated pipette and shown on the graphs in Results. The 100-1000 μL micropipette had a 3 μL uncertainty, but as the data is graphed categorically, the uncertainty is not shown. The uncertainty in temperature acquisition has been previously reported by the EDL to be 2.2°C and was also used for this investigation.

3 Results

3.1 Visualization of results

The results of experimentation for both aromatic content and branching are expressed in the form of an ignition map (Figures 11 and 17). This ignition map shows which form of ignition or non-ignition occurred at each temperature for each type of fuel, allowing for analysis of boundaries of ignition. In addition to the ignition maps, the T4 temperature probe signals for all tests are also shown, except for 20% TMB, 30% TMB, and 2,2,4,4-tetramethylpentane, which use representative graphs. Finally, the activation energy of combustion for three of the four aromaticity fuels has been found according to the method explained below.

The testing for branching began with the intention of finding the boundaries of the ignition modes. However, certain phenomena occurred that made it difficult to define ranges for modes of ignition. Thus, the data is presented to accommodate these differences, highlighting the missing information needed to confidently categorize the results. Discussion on how this information might be acquired in future testing is also included in the Conclusions.

3.2 Aromatic content results

3.2.1 Summary of aromatic content results

The experimental results for the aromaticity testing provide critical insights into the behavior of a fuel as the aromatic content is increased. The ignition map below clearly delineates the transition between the different ignition modes at different ignition temperatures (Figure 11). By comparing the boundary between Mode IV and Mode III, it can be seen that higher TMB content pushes the boundary to a higher temperature. These boundaries are expressed numerically in Table 5.

However, it should be noted that these boundaries are not well defined, as demonstrated by the ignition case at ~217°C for 20% TMB despite several non-ignition tests at higher temperatures. There could be many reasons for this beyond the statistical behavior of ignition discussed in [5], such as the presence of gas in the syringe or the flask temperature not being completely stable.

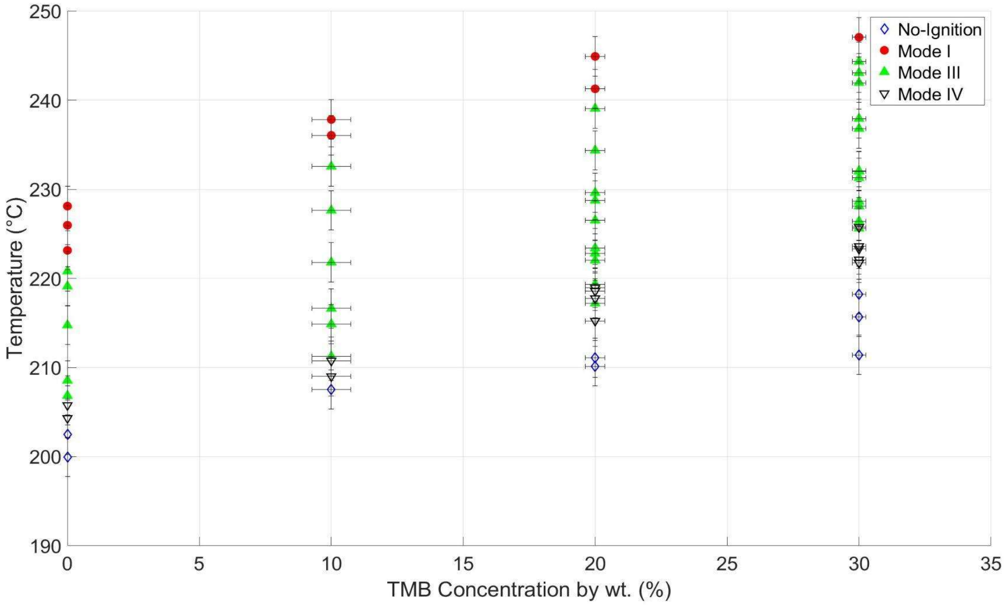

Figure 11: Ignition map for the four different component fuels used to investigate the effect of aromatic content on AIT. The boundary from black to green is the AIT, while the boundary from green to red is the transition from Mode III ignition to Mode I. The boundary temperature increases as TMB content increases.

Fuel	AIT: Mode IV → Mode III (±2.2°C)	Mode III → Mode I (±2.2°C)
0% TMB	205.8 - 206.8 (~206)	220.8 - 223.1 (~222)
10% TMB	210.8 - 211.3 (~211)	232.6 - 236.0 (~234)
20% TMB	218.6 - 219.4 (~219)	239.1 - 241.3 (~240)
30% TMB	225.7 - 226.4 (~226)	244.3 - 247.1 (~245)

Table 5: Temperature ranges (°C) for the boundaries between ignition modes. The boundaries are the highest temperature at which one mode occurred and the lowest at which the next one occurred. Written alongside these ranges is an average value that can be used to represent the boundary location.

3.2.2 Individual aromatic content fuel graphs

Figures 12 to 15 display the temperature signals from the T4 temperature probe vs. time for each fuel tested during the aromaticity experimentation. In the legend is the test number, the initial temperature, the maximum temperature as described in methods, and the mode of ignition. 20% TMB and 30% TMB only show representative signals to decrease clutter and express the boundary of modes of ignition, all data are graphed in Appendix A.

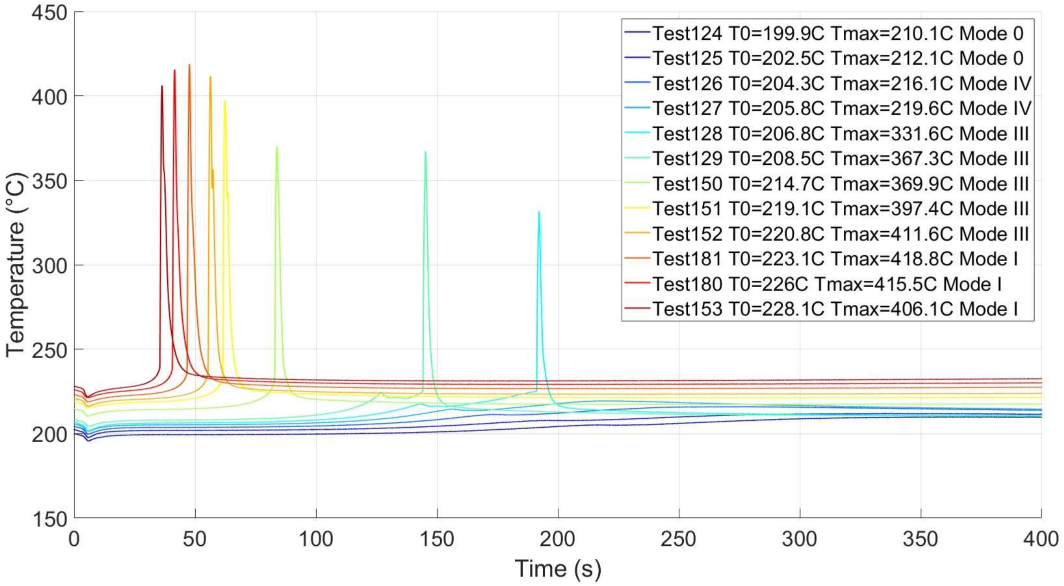

Figure 12: Temperature signals for all 0% TMB (pure n-nonane) tests. The boundaries between modes are given in Table 5.

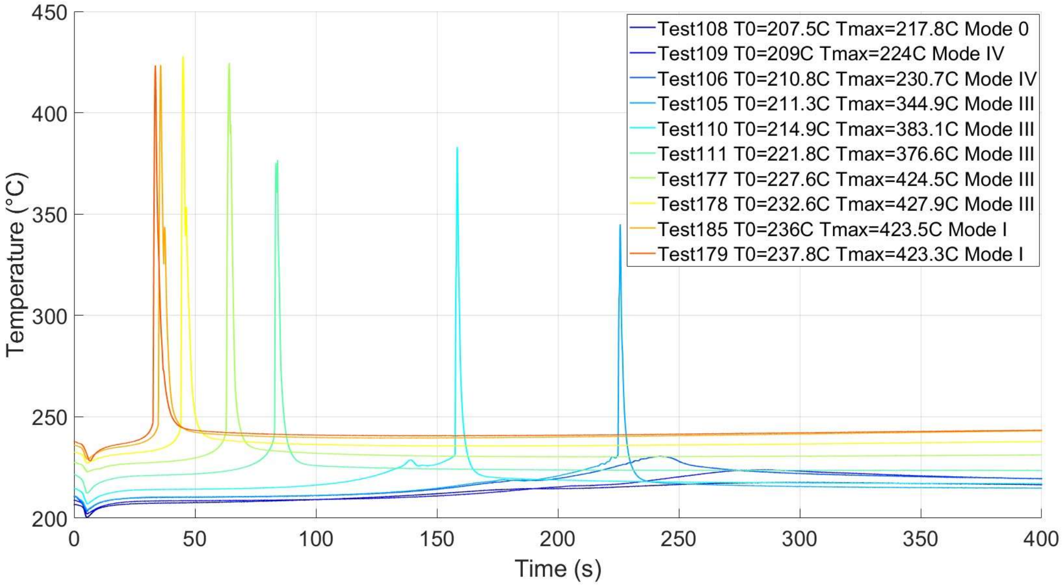

Figure 13: Temperature signals for all 10% TMB tests. The boundaries between modes are given in Table 5. One artifact to note is the presence of a smaller preliminary peak in Test 110, the second Mode III peak from the right. These smaller peaks occur more than once throughout testing as explained in the Discussion.

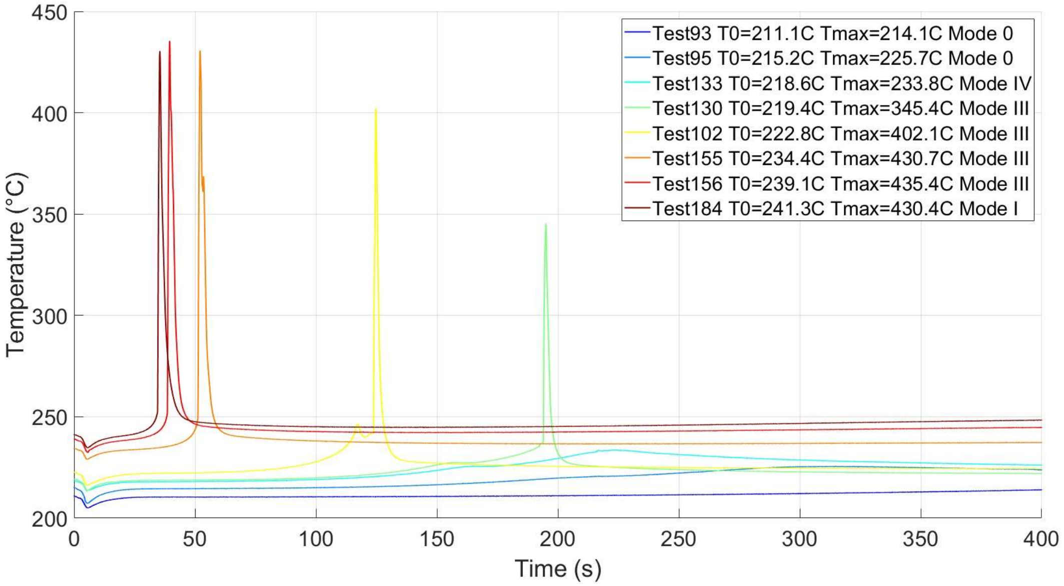

Figure 14: Graph of representative 20% TMB ignition signals that emphasize the boundaries between the various modes of ignition. The graph of T4 temperature signals for all 20% TMB tests can be found in Appendix A (Figure A1).

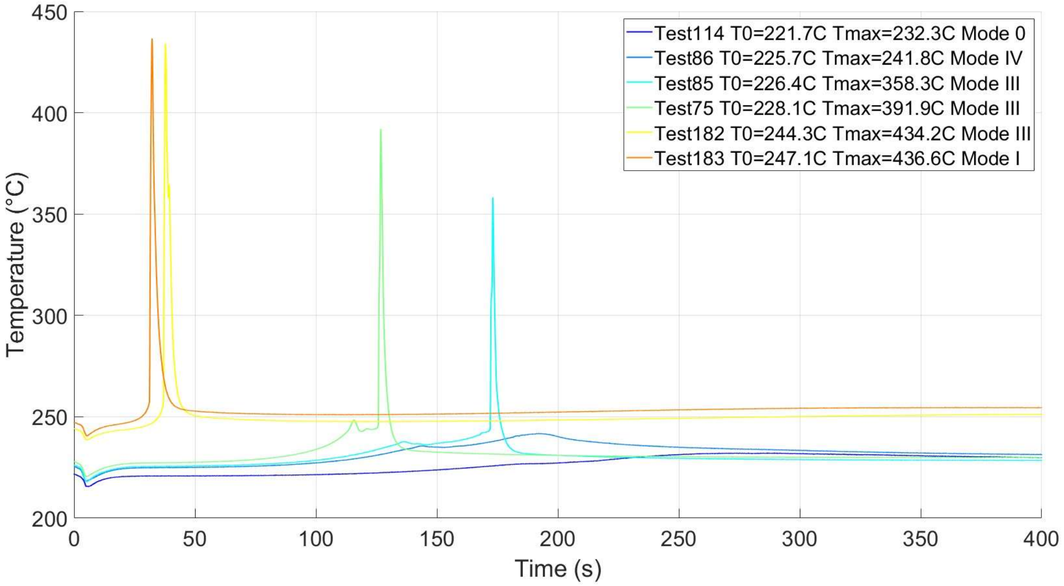

Figure 15: Graph of representative 30% TMB ignition signals that emphasize the boundaries between the various modes of ignition. The graph of T4 temperature signals for all 30% TMB cases can be found in Appendix A (Figure A2).

3.2.3 Activation energies

It is possible to use the ignition delay times and the initial temperatures of several tests for a fuel spread out over various temperatures to find the effective activation energy of combustion for that fuel. As discussed in Fouchier and Shepherd [5], the Arrhenius equation for ignition delay time is:

$$\tau_i = ae^{\frac{Ea}{RT}} \tag{1}$$

where τ_i is the ignition delay time, a is the pre-exponential factor, Ea is the activation energy in joules per mole, R is the universal gas constant ($8.314\,\frac{\mathrm{J}}{\mathrm{mol}}\cdot\mathrm{K}$), and T is the absolute temperature in kelvins (K).To linearize this equation, we take the natural logarithm of both sides:

$$ln\,(\tau_i) = ln\,(a) + \frac{-Ea}{R} \cdot \frac{1}{T} \tag{2}$$

By performing a linear regression on the data points $ln\,(\tau_i)$ versus $\frac{1}{T}$, the slope of the resulting line can be used to calculate the activation energy. Specifically, the slope is equal to $\frac{-E}{R}$, so the activation energy can be computed by multiplying the slope by -R and multiplying by 1000 to get the activation energy in units of kJ/mol.

$$Ea = -\mathrm{slope} \times R \times 1000, \frac{\mathrm{kJ}}{\mathrm{mol}} \tag{3}$$

Using the method described above, the Arrhenius plots of 0%TMB, 20%TMB, and 30%TMB have been presented on the same graph alongside the calculated activation energy for each (Figure 16). 10% TMB did not have enough ignition cases for a meaningful Arrhenius plot. While the difference in *Ea* for 30% and 20% TMB is not large enough to be significant, the jump from 0% TMB *Ea* shows *Ea* increases with increasing aromatic content.

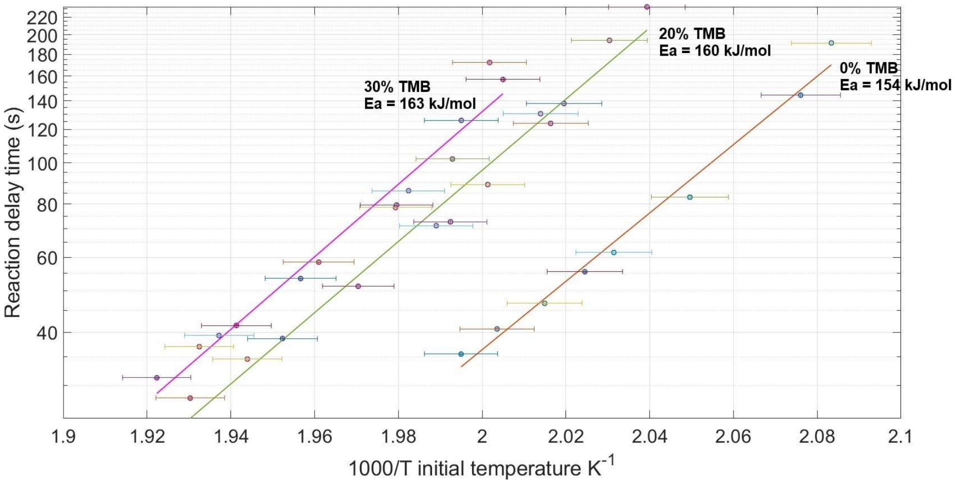

Figure 16: Arrhenius plots for the ignition cases of 0%, 20%, and 30% TMB.

3.3 Branching results

3.3.1 Summary of branching results

The experimental results for the branching testing are not as clear-cut as the results from the aromaticity investigation. The ignition map and table showing the empirical boundaries of ignition are given in Figure 17 and Table 6. The initial hypothesis –that branching would increase AIT– is not supported when comparing n-nonane and 2-methyloctane as fuel components. The n-nonane component fuel experienced Mode III ignition at 239.1 ±2.2°C and 2-methyloctane experienced Mode I at 239.0 ±2.2°C (Table 6). Only a few tests were done for 2-methyloctane, and the difference is within the uncertainties, so it isn't possible to make a definite statement regarding a higher or lower AIT. Further investigation can clarify exactly where is the boundary between Mode III and Mode I ignition for the 2-methyloctane component fuel. The location of this boundary does not support the prediction that adding a methyl group would increase the AIT.

The differences in AIT between 2-methyloctane and 2,2,4-trimethylhexane substantially exceed the uncertainty limits in the measurements (Table 6). Thus, it can be inferred that the highly branched structure of 2,2,4-trimethylhexane and 2,2,4,4-tetramethylpentane increase the component fuel AIT compared to n-nonane and 2-methyloctane. However, without the 2,3-dimethylheptane data, the influence of each subsequent methyl group addition is difficult to ascertain.

A peculiar trend was found when investigating the 2,2,4-trimethylhexane component fuel and is magnified in Figure 20. There appears to be two peaks or temperature excursion representing exothermic reactions that converge as the temperature increases until forming a much shallower excursion. With increasing temperature, Mode I ignition occurs with a visible flame. Even during the most exothermic test before merging into one peak (Test 143), there was no visible flame or puff of smoke to the naked eye. These peculiarities are further discussed in Figures 20 and 21, and in the branching subsection of the Discussion.

Finally, the boundaries of ignition for 2,2,4-trimethylhexane and for Mode I ignition of 2-methyloctane are not precise enough (within uncertainties) to give a single temperature value for the autoignition temperature. In particular, the Mode IV → Mode I boundary of 2,2,4-trimethylhexane, if averaged, would be higher than the respective boundary for 2,2,4,4-tetramethylpentane. However, indicating that this boundary is at a higher temperature for 2,2,4-trimethylhexane would be misleading and is not supported by the data, thus the average for this boundary and other ones mentioned have been omitted from Table 6.

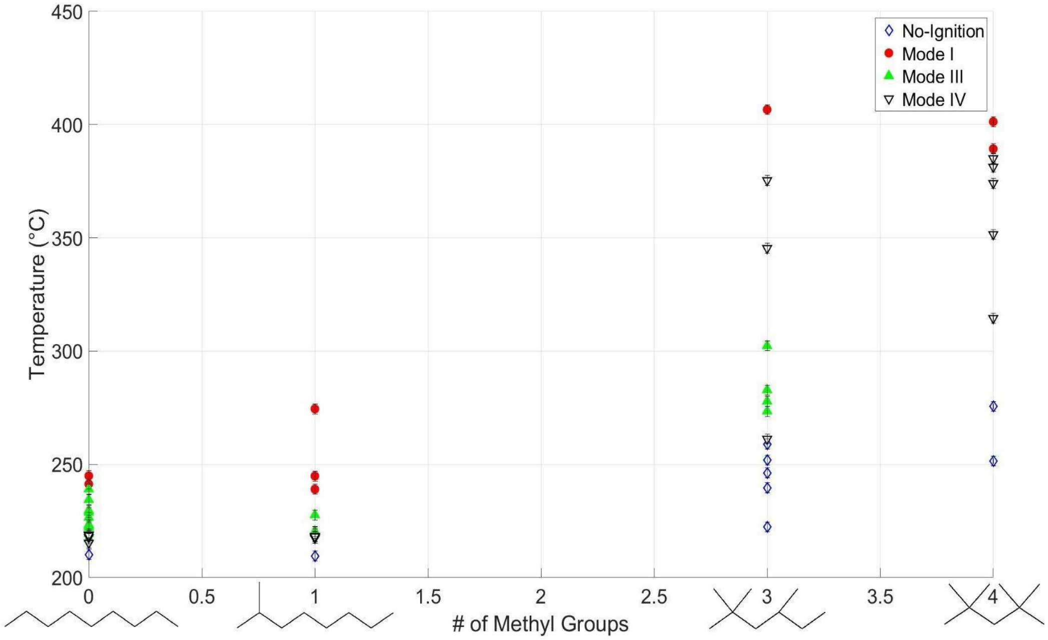

Figure 17: Ignition map for the four two-component fuels used to investigate the effect of branching on AIT. Beneath each category is the molecular structure of "Component 1" corresponding to the # of methyl groups (Tables 2 and 4). The boundaries are articulated below in Table 6.

Fuel	Boundary (±2.2°C)	Boundary "Type"
n-nonane	218.6 - 219.4 (~219)	Mode IV → Mode III
	239.1 - 241.3 (~240)	Mode III → Mode I
2-methyloctane	218.3 - 219.4 (~219)	Mode IV → Mode III
	227.6 - 239.0	Mode III → Mode I
2,2,4-trimethylhexane	261.2 - 273.4	Mode IV → Mode III
	375.4 - 406.7	Mode IV → Mode I
2,2,4,4-tetramethylpentane	385.1 - 389.3 (~387)	Mode IV → Mode I

Table 6: Boundaries between ignition modes found during the branching investigation (Figure 17). A boundary column type has been added rather than having Mode IV → Mode III and Mode III → Mode I columns like with aromaticity (Table 5) because the boundaries are not the same for the tested fuels.

3.3.2 Individual branching fuel graphs

Figures 14, 18, 19, and 22 show temperature signals from the T4 temperature probe for each fuel tested during the branching content experimentation. In the legend is the test number, the initial temperature, maximum temperature as described in Methods, and the mode of ignition. Results of the 2,2,4-trimethylhexane component fuel testing had peculiar temperature signals. Between 258.9 ±2.2°C and 261.2 ±2.2°C, there are indications of a substantial exothermic reaction, and long-duration, low-amplitude rise following the initial peak (Figure 20). This rise becomes more acute as the temperature increases while the temperature increase from the first peak decreases. These results deviate from the results commonly found with other fuels (Figure 21), and the implications are explored in the Discussion.

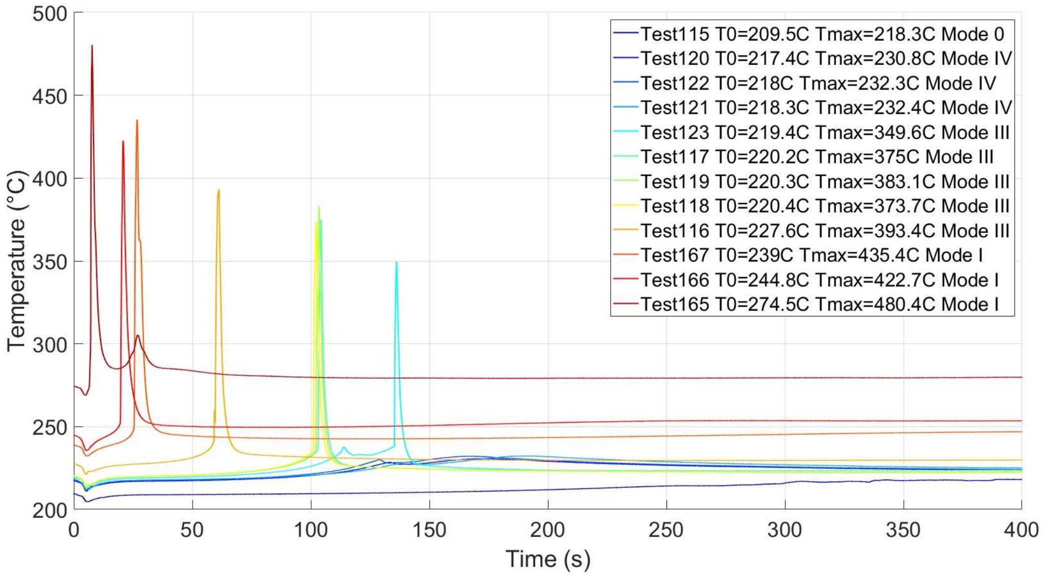

Figure 18: Temperature signals for all 2-methyloctane component fuel tests. The boundaries are described in Table 6.

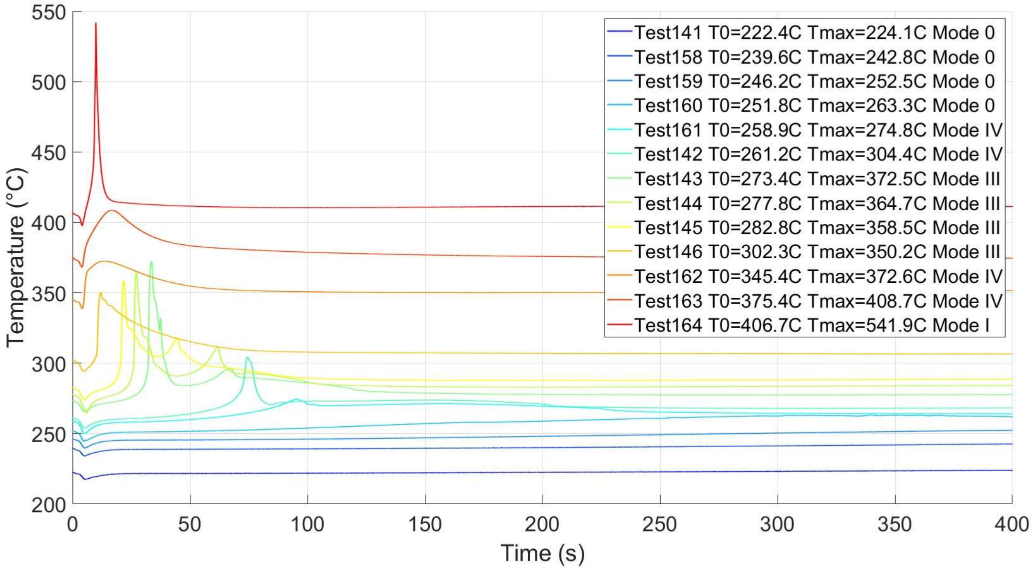

Figure 19: Temperature signals for all 2,2,4-trimethylhexane component fuel tests. The boundaries are described in Table 6. A further investigation into the anomalous first boundary between Mode IV rapid reaction and Mode III ignition is shown in the figure below.

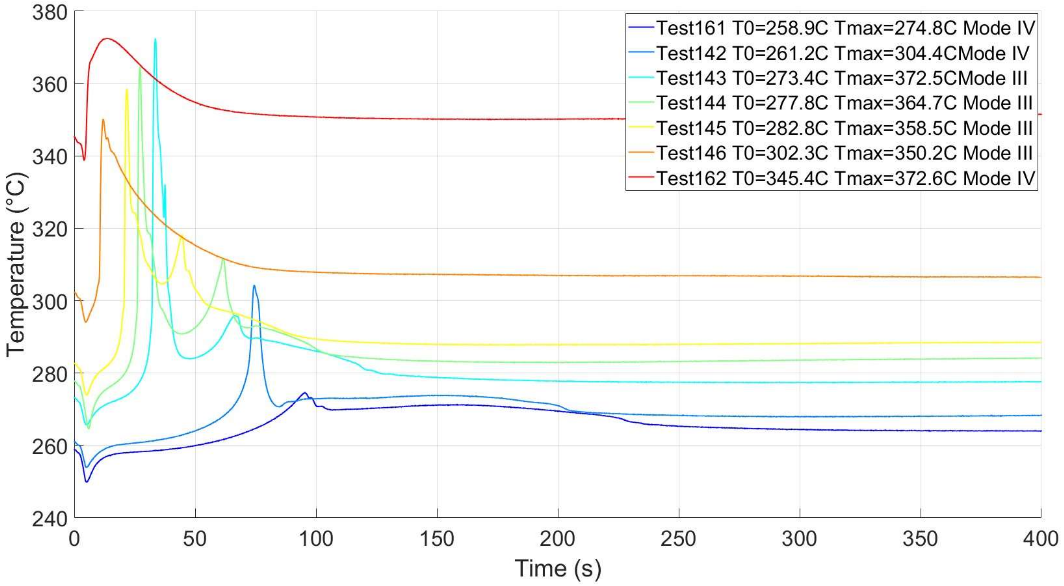

Figure 20: 2,2,4-trimethylhexane "first boundary". The irregular relationship between initial temperature and peak temperature change is shown graphically in Figure 21.

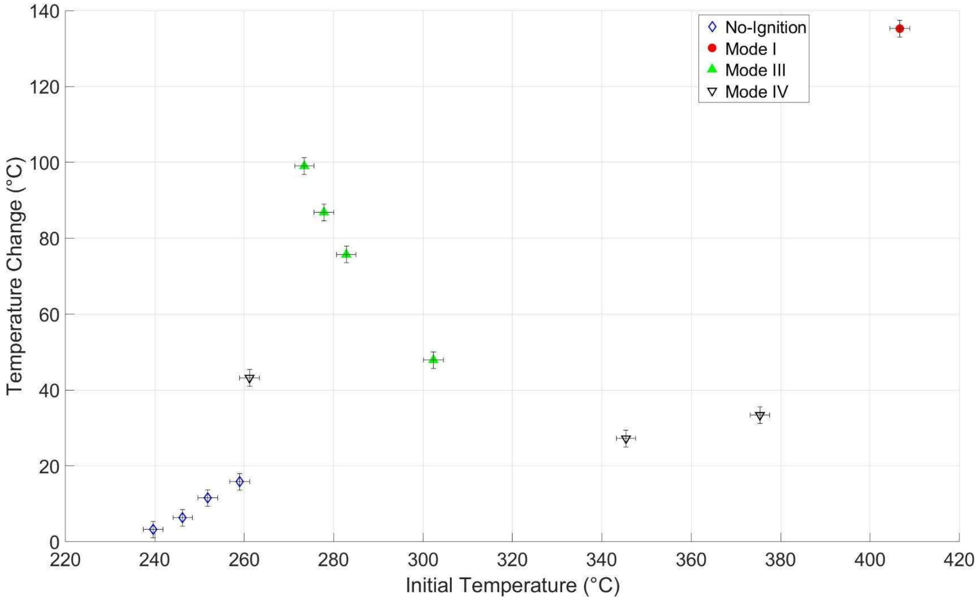

Figure 21: Maximum temperature recorded by the T4 thermocouple as a function of the initial temperature for 2,2,4-trimethylhexane. Similar graphs for other fuels can be found in Appendix A (Figures A4 and A5) to show the irregularity of 2,2,4-trimethylhexane.

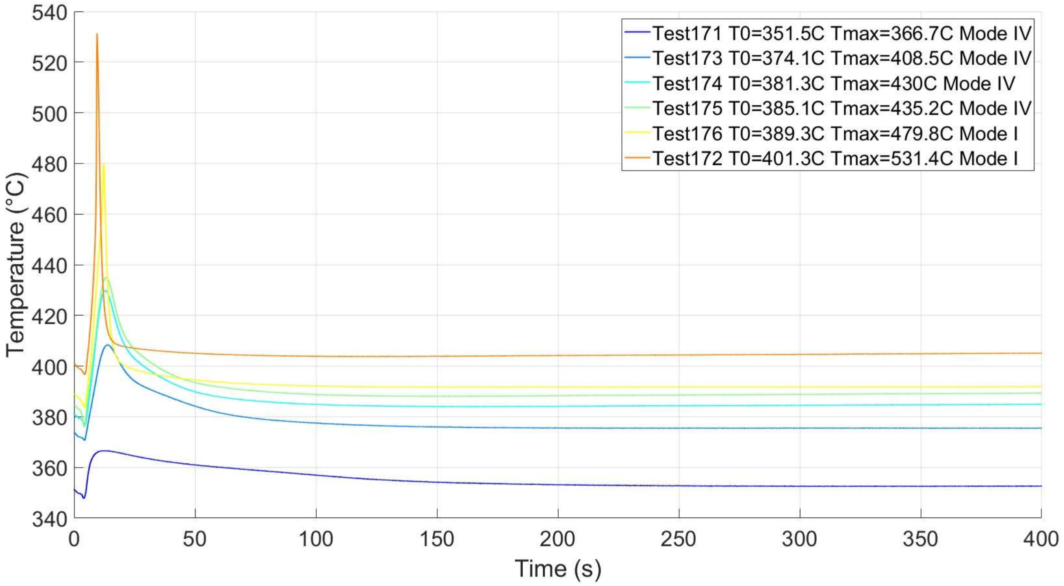

Figure 22: Temperature signals for representative 2,2,4,4-tetramethylpentane component fuel tests. The boundaries can be found described above in Table 6. Some tests have been omitted to improve clarity; the full graph is available in Appendix A (Figure A3).

4 Discussion

4.1 Modes of ignition

One notable observation regarding modes of ignition found in this experiment is the lack of Mode II ignition. Mode II ignition has been previously observed when testing certain fuels such as TMB, iso-cetane, trans-decalin, and toluene [3], [8]. Further investigation into the presence of Mode II ignition will require observation with a photodiode or camera, as Mode II ignition has a glow so dim it isn't visible to a human eye unless dark-adapted in a pitch-black room.

The mode of ignition is dependent on the volume of the fuel injected. In testing with Jet A and SPK, previous testing found that larger volumes (600 µL) tend to favor Mode I ignition while smaller volumes (100 µL) favor Mode III ignition. A volume of 300 µL was used in all of the present tests which may bias the determination of the mode boundaries.

4.2 Aromatic content

There is an increase in AIT as an aromatic compound, TMB, is added to a straight chain molecule with a comparatively low autoignition temperature, n-nonane. Substituting 10 wt% of the nonane with TMB causes a ~5 ±2.2°C increase in the boundary between Mode IV and Mode III ignition. There are several ways this could be further investigated. To investigate whether the aromaticity or the high (515°C) AIT of TMB are factors, the experiment can be repeated without an aromatic molecule and a high AIT, non-aromatic hydrocarbon, such as iso-cetane. If a reliable detailed chemical reaction mechanism is available, the experimentation could be supplemented and interpreted with numerical simulation of the reaction process.

This preliminary investigation suggests that the lack of aromatic components in the SPK reduces the AIT compared to commodity aviation kerosene (Jet A). There are other differences between SPK and Jet A [5], these may also be factors in determining the AIT.

4.3 Branching

This preliminary investigation suggests that a highly branched compound may also increase the AIT relative to straight chain compounds. Comparing the fuel with 80 wt% 2-methyloctane to the fuel with 80 wt% 2,2,4-trimethylhexane shows a minimum 20 ±2.2°C increase in AIT even when considering the peculiarity of the 2,2,4-trimethylhexane ignition. This effect is even more drastic with 2,2,4,4-tetramethylpentane which doesn't exhibit the peculiar low-temperature exothermic reactions of 2,2,4-trimethylhexane.

An important next step could be to answer the questions raised by the unusual temperature signals with 2,2,4-trimethylhexane (Figures 20 and 21). The dual peak artifact noted in 2,2,4-trimethylhexane and in other tested component fuels indicate that defining low-temperature autoignition is more subtle than just ignition vs. no ignition. One possibility to explain the double peaks that eventually merge is the possibility of competing reactions, which could be explored through numerical simulation as mentioned previously. Refinements in experimental methods using more sensitive (photodiodes or cameras) measurements could quantity possible Mode II ignition. Further systematic testing with non-aromatic hydrocarbons, alone or in mixtures with other fuel blends such as SPK, may be useful in examining the role of branching in molecular structure on AIT. Developing a deeper understanding of the reaction processes behind modes of ignition, double peaks, and other phenomena will be important in synthesizing fuels with known AITs.

5 Conclusions and future work

Utilizing the automated EDL ASTM-E659 apparatus, a systematic study was performed to determine the effect of molecular structure on AIT for two representative fuel blends. Two component mixtures were formulated to separately test the effect of aromatic content and number of branches for alkane isomers. The results show that increasing the aromatic content increases the AIT. The lower AIT in SPK as compared to Jet A may be due to the lack of any aromatic molecules in SPK [5]. The results show that highly branched isomers have a higher AIT than straight chain alkanes, but the temperature signals are unusual for the highly-branched compounds and require further investigation.

However, the limitations of the present study should be considered in deciding future research directions. In particular, the branching study could be improved by determining the ignition boundaries of a mixture consisting of 80 wt% 2,3-dimethylheptane and 20 wt% TMB. After filling in the missing 2,3-dimethylheptane data point, if the results corroborate branching as a means to increase AIT, the next step would be studying the effects of replacing the aromatic compound with something like 2,2,4-trimethylhexane. Testing fuels with increasing branched wt%, like what was done in the aromatic content testing, would provide the means to compare TMB to a highly branched, non-aromatic additive. Another issue is the need for better instrumentation to monitor the presence of light in the flask to evaluate the possibility of Mode II ignition in some tests. Such improvements could be used in further investigation regarding the double peaks found in some of the fuels tested, especially 2,2,4-trimethylhexane.

Despite the limitations of the present study, much valuable insight was obtained into the role of the aromatic content and branching amount of isomer. The tests demonstrated the repeatability of the automated ASTM apparatus and the utility of the 75 Hz recording of the temperature signals in analyzing ignition events.

6 Acknowledgements

I would like to extend my gratitude to the Caltech SURF program. I also would like to thank the Explosion Dynamics Laboratory and the Boeing Company for financial support. I would like to thank Professor Joe Shepherd who provided me an opportunity to work in his lab, and Dr. Charline Fouchier, who provided much needed guidance throughout the project. I would also like to thank the Dr. Chandler C. Ross SURF fellowship as well as the SFP office at Caltech for funding my SURF project.

7 References

[1] ASTM, “ASTM-E659-14: Standard test method for autoignition temperature of liquid chemicals.” ASTM International, 2005.

[2] W. A. Affens, J. E. Johnson, and H. W. Carhart, “Effect of Chemical Structure on Spontaneous Ignition of Hydrocarbons.,” *J. Chem. Eng. Data*, vol. 6, no. 4, pp. 613–619, Oct. 1961, doi: 10.1021/je60011a041.

[3] C. D. Martin and J. E. Shepherd, “Low temperature autoignition of Jet A and surrogate jet fuel,” *J. Loss Prev. Process Ind.*, vol. 71, p. 104454, Jul. 2021, doi: 10.1016/j.jlp.2021.104454.

[4] F. Battin-Leclerc, “Detailed chemical kinetic models for the low-temperature combustion of hydrocarbons with application to gasoline and diesel fuel surrogates,” *Prog. Energy Combust. Sci.*, vol. 34, no. 4, pp. 440–498, Aug. 2008, doi: 10.1016/j.pecs.2007.10.002.

[5] C. Fouchier and J. Shepherd, “ASTM E659 Standardized Test Analysis and Results for Synthetic Paraffinic Kerosene,” 15th International Symposium on Hazards, Prevention and Mitigation of Industrial Explosions, Naples, ITALY – June 10-14, 2024.

[6] AIChE, “Evaluated process design data, Design Institute for Physical Properties Relationships (DIPPR) Project 801.” 2009. [Online]. Available: https://www.aiche.org/dippr/about

[7] C. L. Yaws, *Chemical Properties Handbook: Physical, Thermodynamics, Environmental Transport, Safety & Health Related Properties for Organic &*. McGraw-Hill Education, 1999.

[8] S. Honnet, K. Seshadri, U. Niemann, and N. Peters, “A surrogate fuel for kerosene,” *Proc. Combust. Inst.*, vol. 32, no. 1, pp. 485–492, 2009, doi: 10.1016/j.proci.2008.06.218.

8 Supplemental materials

Preliminary Excel File

Appendix A

Appendix B

Appendix A

Appendix Creator: Colin Gray
Last Modified: September 9th, 2024

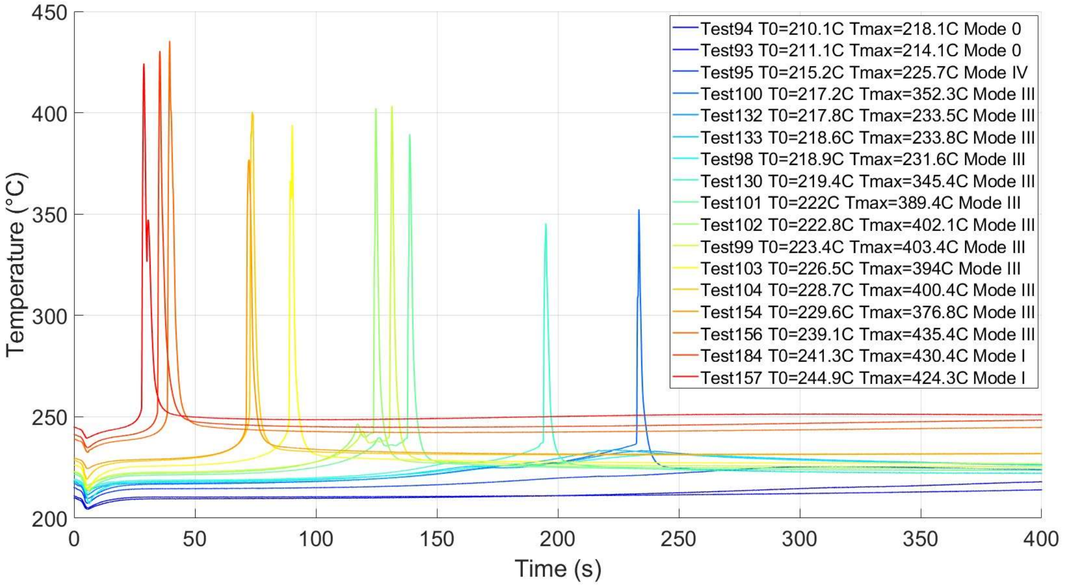

Figure 1A: All 20% TMB test T4 temperature signals.

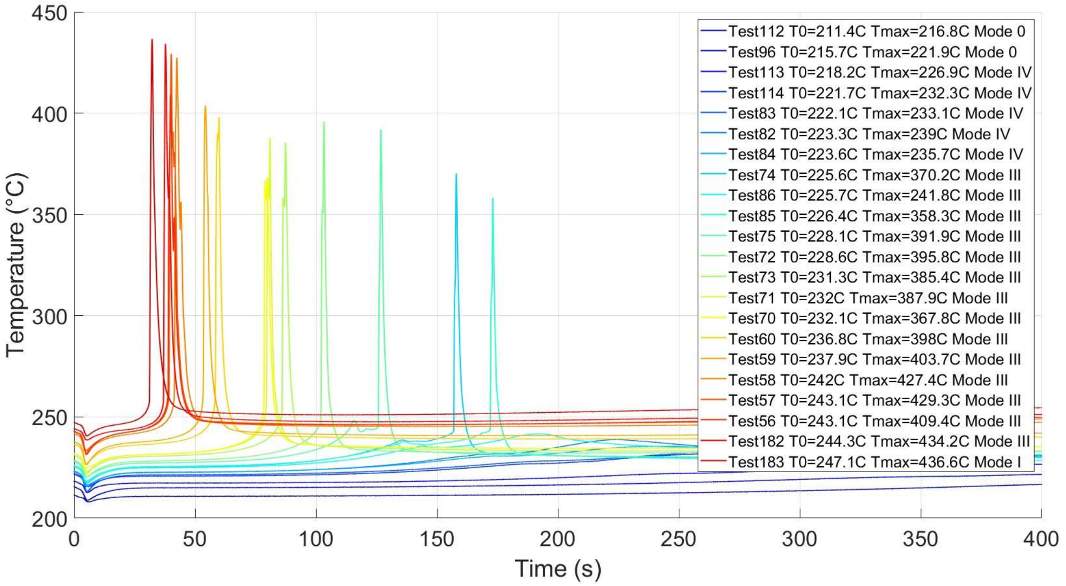

Figure 2A: All 30% TMB test T4 temperature signals.

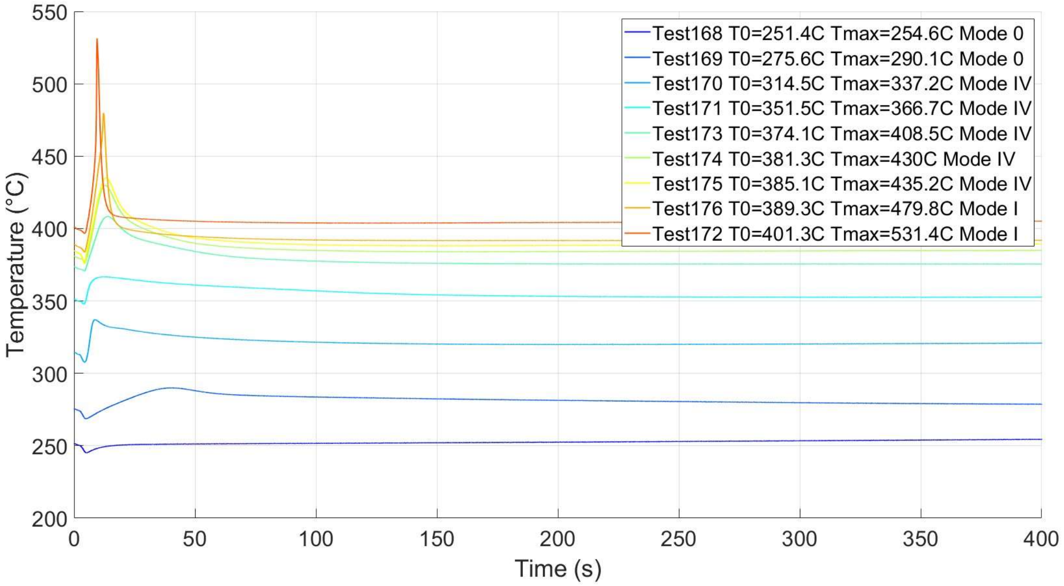

Figure 3A: All 2,2,4,4-tetramethylpentane test T4 temperature signals.

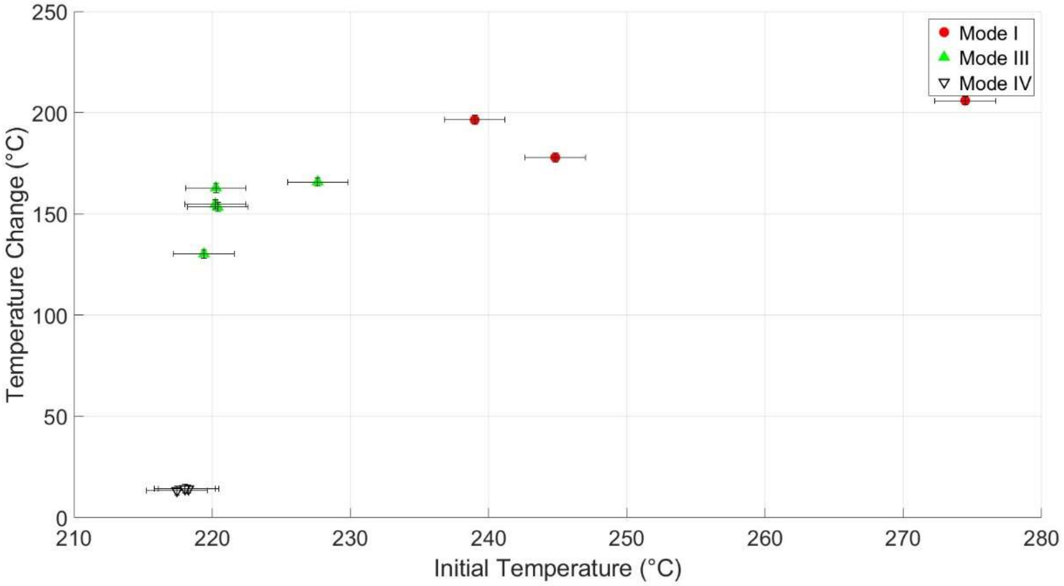

Figure 4A: Temperature change vs. initial temperature for 2-methyloctane. There is no sharp decrease in temperature change as initial temperature increases like there is in 2,2,4-trimethylhexane component fuel test results.

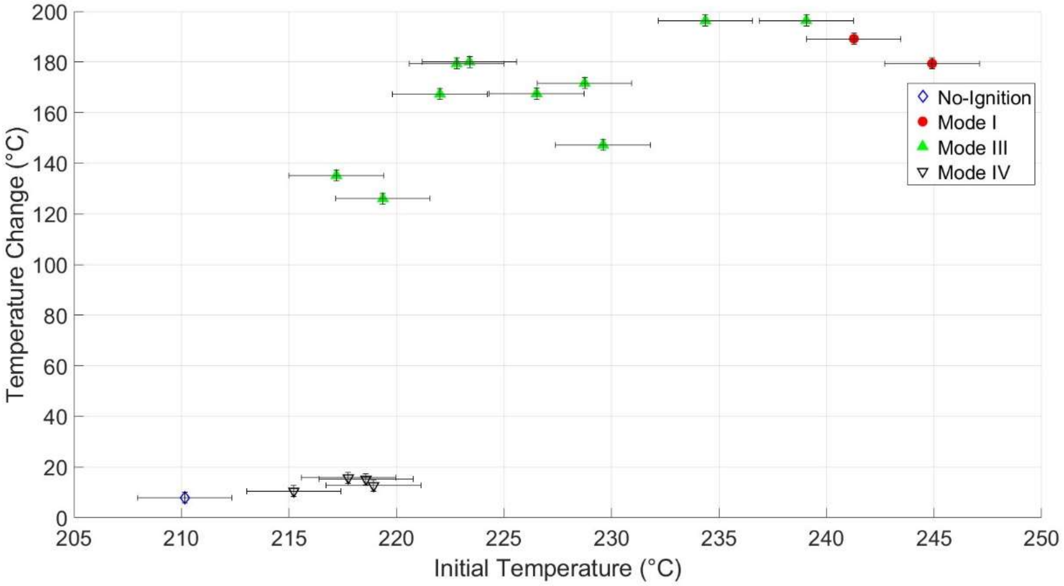

Figure 5A: Temperature change vs. initial temperature for 20% TMB (n-nonane in aromaticity testing). Once again, there isn't the same period of significant decreasing in temperature change as initial temperature increases.

Appendix B

Appendix Creator: Colin Gray
Last Modified: September 9th, 2024

AUTHOR NOTE: “Base” molecule is just a subjective quality to group molecules based on how the “backbone” is augmented. So, everything within the hexane group has a straight chain hexane as the longest hydrocarbon chain, or cyclohexane is any molecule with hydrocarbons branching off of a cyclohexane, etc.

DISCLAIMER 1: These are just some of the many graphs investigated correlating AIT to hydrocarbon structure. They were merely created to find possible correlations, whether weak or strong. As such, the graphs are directly saved from Excel and have minimal formatting, but representative molecules have been made and added to the graphs to provide some insight into what certain graphs are representing. That being said, some graphs essentially say the same thing, like length of substituent and number of substituent graphs are almost the same as size of molecule if grouped by like “base.”

DISCLAIMER 3: Much of this data has very large uncertainties as it is estimated using algorithms from the DIPPR database. Once again, these graphs and the data found in the Preliminary Excel File were all simply to find direction.

DISCLAIMER 2: All Data is from the following sources as indicated in the Preliminary Excel File under Supplementary Materials:

[1] W. A. Affens, J. E. Johnson, and H. W. Carhart, “Effect of Chemical Structure on Spontaneous Ignition of Hydrocarbons.,” *J. Chem. Eng. Data*, vol. 6, no. 4, pp. 613–619, Oct. 1961, doi: 10.1021/je60011a041.

[2] AIChE, “Evaluated process design data, Design Institute for Physical Properties Relationships (DIPPR) Project 801.” 2009. [Online]. Available: https://www.aiche.org/dippr/about

[3] C. L. Yaws, *Chemical Properties Handbook: Physical, Thermodynamics, Environmental Transport, Safety & Health Related Properties for Organic &*. McGraw-Hill Education, 1999.

As all data has been attached in the Preliminary Excel File, it is possible to add more columns and attempt to find other correlations, the ones that have been attached are just a handful of what was created, primarily the only ones that showed a semblance of correlation.

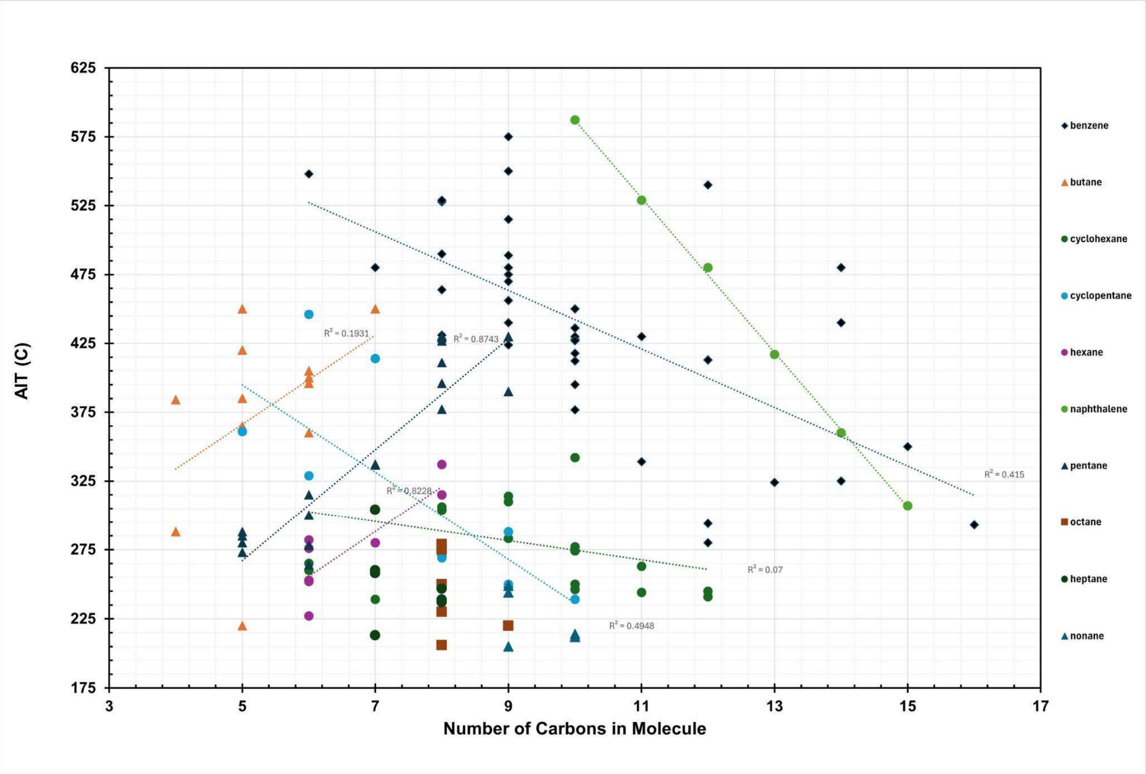

Figure 1B: An investigation into simply whether bigger molecules have higher or lower AIT, grouped by the backbone described in the Author's Note.

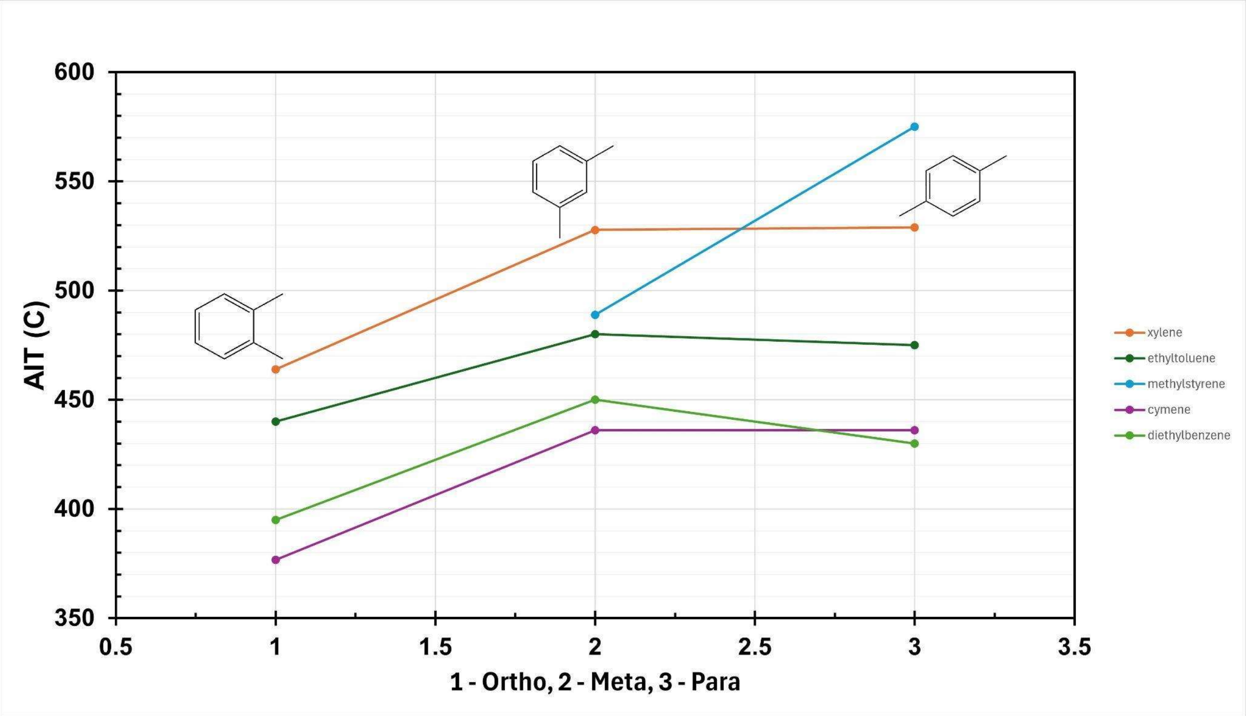

Figure 2B: An investigation into whether the position of substituents on benzene molecules matter, and there is definitely a decrease in AIT if ortho, otherwise not much correlation.

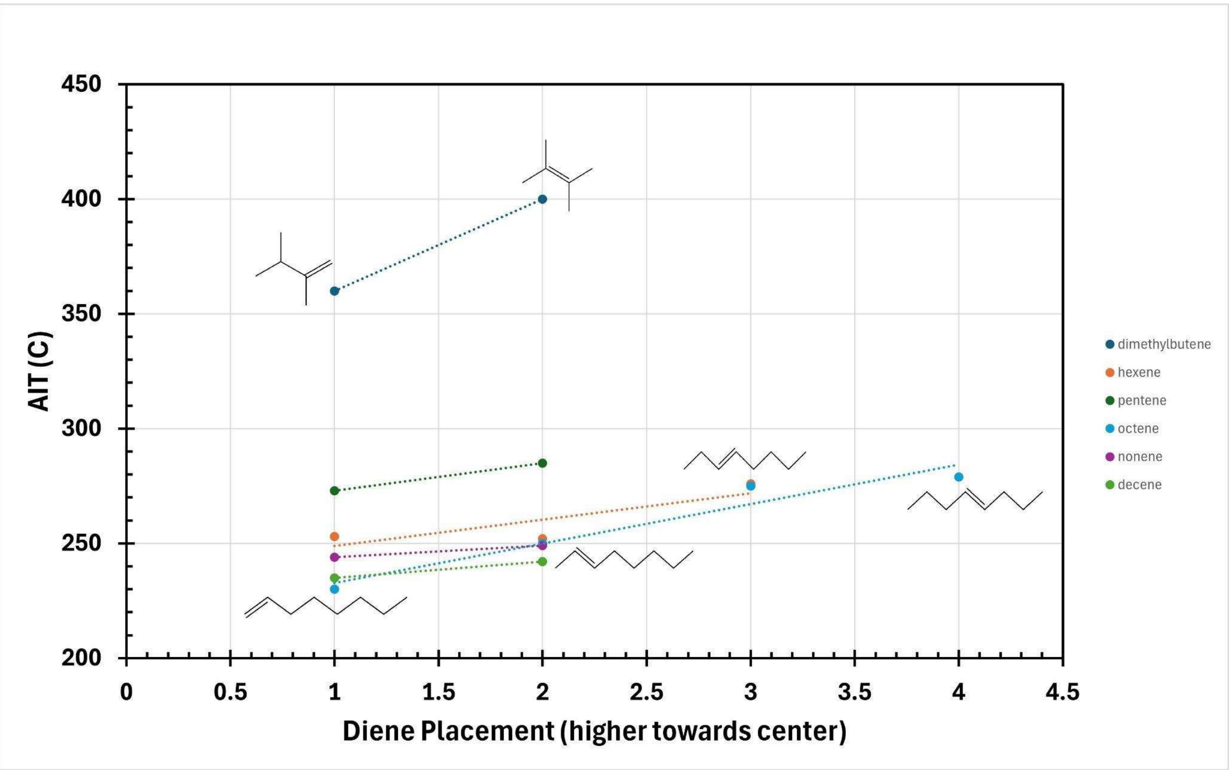

Figure 3B: An investigation into whether the AIT of a single double bond diene will change depending on the position of the double bond relative to the center.

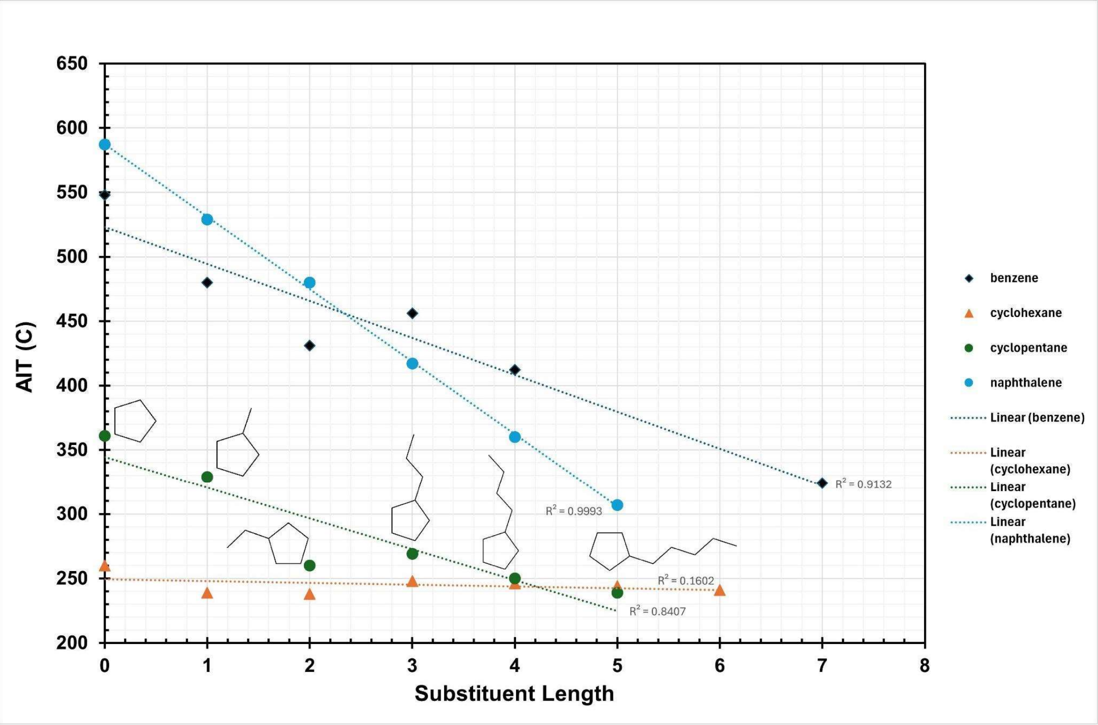

Figure 4B: An investigation into how AIT changes as the length of a substituent increases, essentially showing the same information as the size of hydrocarbon graph.

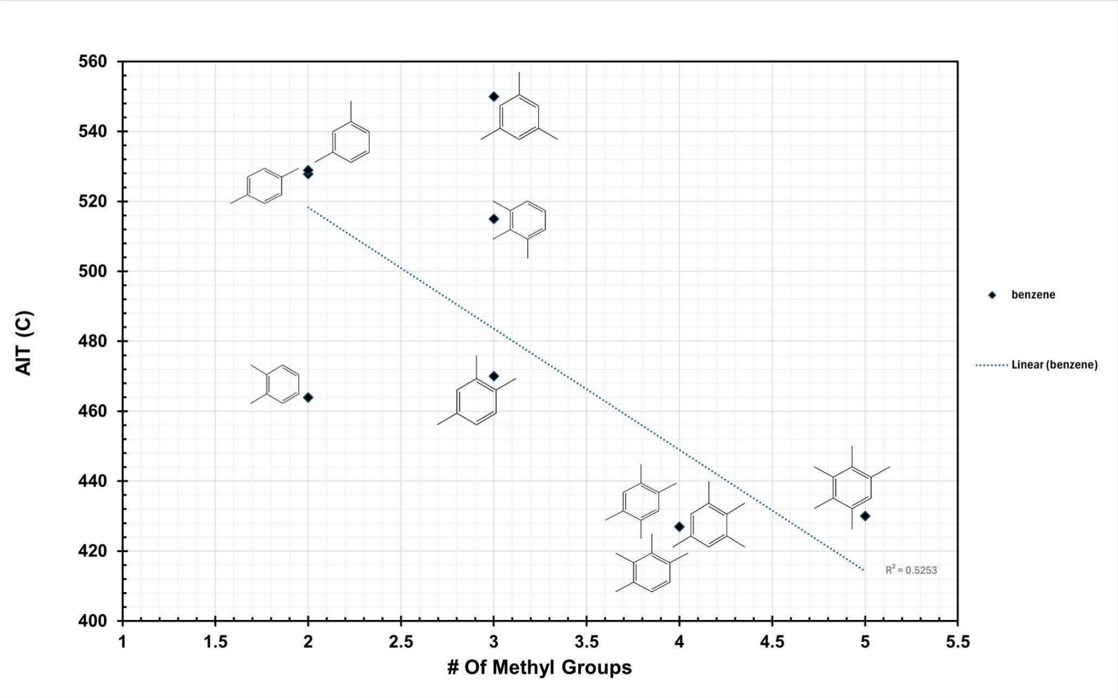

Figure 5B: An investigation into how AIT changes as methyl groups are added to benzene. This graph, and a similar graph with naphthalene imply that the aromatic molecules have higher AIT if there aren't things attached to them. This makes sense when considering that depending on what is attached, the electron conjugation is interrupted.

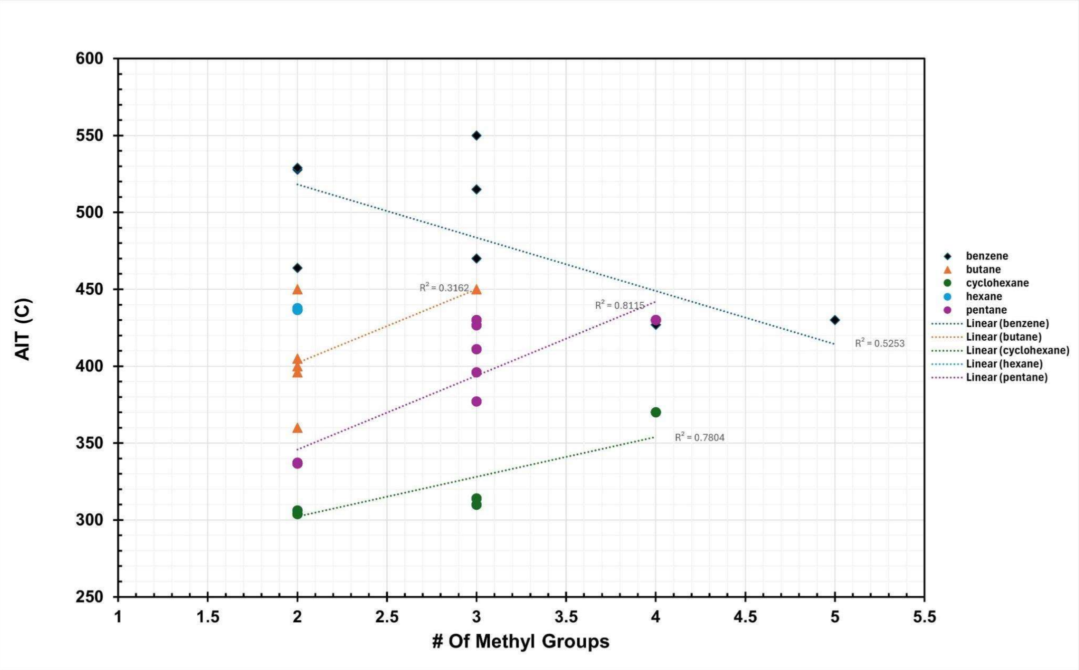

Figure 6B: Same graph as Figure 5B but with other groups added to it. The non-aromatic molecules have a semblance of increasing AIT as methyl groups are added. Not strong enough to warrant investigation in this experiment.

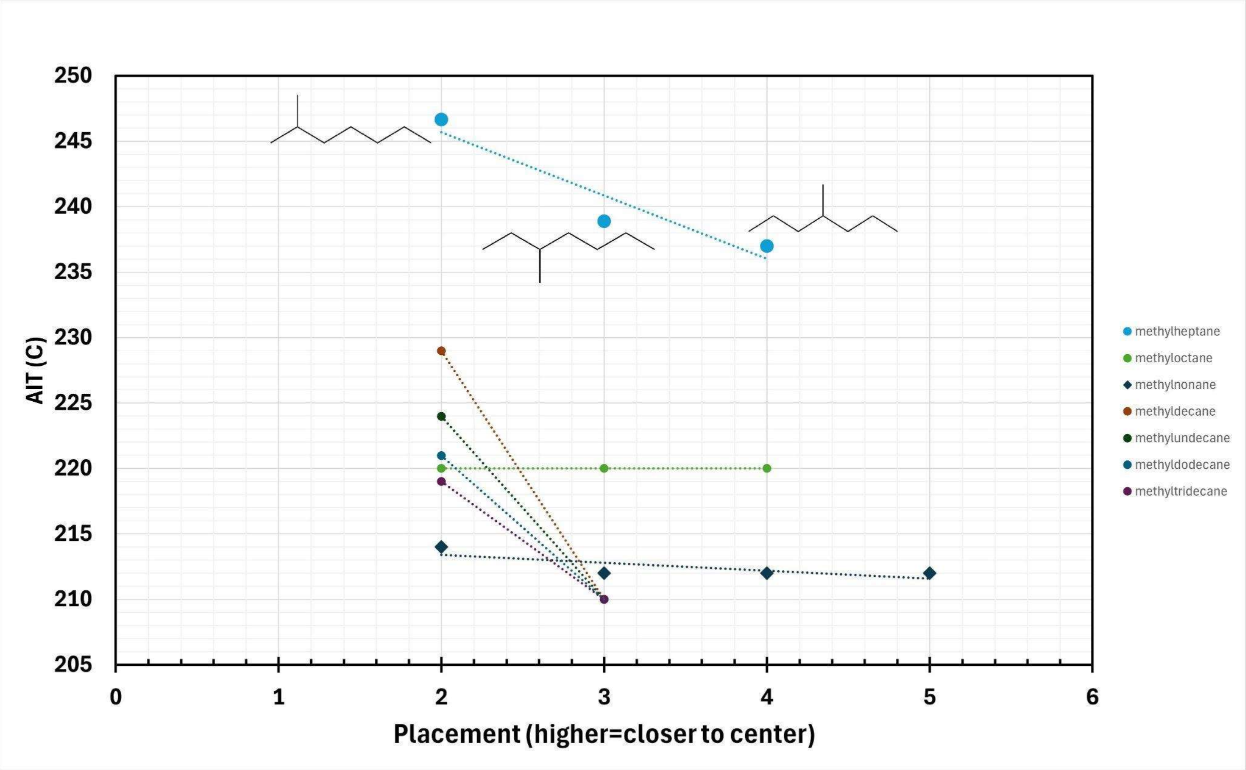

Figure 7B: Another investigation similar to the placement of diene graph, this time with the placement of the methyl group. Several of the molecules had identical AITs, causing the graph to look odd. This is a testament to the precaution needed when using the DIPPR database, and the pitfall of many highly simulated databases.

Preliminary Excel File

On Page 2 of this document is the data acquired from three different sources as well as several "structural" paramatres that aim to provide numerical values to physical hydrocarbon structures allowing for graphing.

REFERENCES FOR AIT INFORMATION: **the AIT blocks are colour coded based on where the information was acquired from** ALL vapour pressure data gathered at 25C from DIPPR website

🟥 C. L. Yaws, Chemical Properties Handbook: Physical, Thermodynamics, Environmental Transport, Safety & Health Related Properties for Organic &. McGraw-Hill Education, 1999.

🟩 W. A. Affens, J. E. Johnson, and H. W. Carhart, “Effect of Chemical Structure on Spontaneous Ignition of Hydrocarbons.,” J. Chem. Eng. Data, vol. 6, no. 4, pp. 613–619, Oct. 1961, doi: 10.1021/je60011a041.

🟦 AIChE, “Evaluated process design data, Design Institute for Physical Properties Relationships (DIPPR) Project 801.” 2009. [Online]. Available: https://www.aiche.org/dippr/about

ALL CREDIT GOES TO THE RESPECTIVE AUTHORS

Data Set Creator: Colin Gray, Caltech
Last Modified: September 9th, 2024

Name	Formula	Number of Carbons	Number of Hydrogens	Classification	Arbitrary #	"Base" General	Diene Placement	Sub Placement	Autoignition Temp C	Number of Substituents	Number of Carbons in Substituents	Percent of Carbons in Substituents	Size of Substituents	Double Bonds (Triple=2)	double bonds (not aromatic)	Double Bonds Not in Substituents	Double Bonds in Substituents	Stereochemistry	substituent position (aromatic)	Butyl		Liquid Vapor Pressure (if found, kPa, @ 25C)
isoprene (2-methyl-1,3-butadiene)	C5H8	5	8	branched (one) (diene)		butane	N/A	N/A	🟥 220	1	1	20.00%	1	2	2	2	0	N/A	N/A	N/A		73.405
1-pentene	C5H10	5	10	straight (diene)		pentane	1	N/A	🟥 273	0	0	0.00%	N/A	1	1	1	0	N/A	N/A	N/A		87.722
n-pentane	C5H12	5	12	straight		pentane	N/A	N/A	🟥 280	0	0	0.00%	N/A	0	0	0	0	N/A	N/A	N/A		68.4
trans-2-pentene	C5H10	5	10	straight (diene)		pentane	2	N/A	🟥 285	0	0	0.00%	N/A	1	1	1	0	trans	N/A	N/A		67.43
cis-2-pentene	C5H10	5	10	straight (diene)		pentane	N/A	N/A	🟥 288	0	0	0.00%	N/A	1	1	1	0	cis	N/A	N/A		65.822
cyclopentane	C5H10	5	10	cyclic		cyclopentane	N/A	N/A	🟩 361	0	0	0.00%	N/A	0	0	0	0	N/A	N/A	N/A		42.333
2-methyl-1-butene	C5H10	5	10	branched (one) (diene)		butane	N/A	2	🟥 385	1	1	20.00%	1	1	1	1	0	N/A	N/A	N/A		81.31
3-methyl-1-butene	C5H10	5	10	branched (one) (diene)		butane	N/A	3	🟥 385	1	1	20.00%	1	1	1	1	0	N/A	N/A	N/A		120.33
isopentane	C5H12	5	12	branched (one)		butane	N/A	N/A	🟥 420	1	1	20.00%	1	0	0	0	0	N/A	N/A	N/A		91.712
neopentane	C5H12	5	12	branched (two)		butane	N/A	N/A	🟥 450	2	2	40.00%	1	0	0	0	0	N/A	N/A	N/A		171.47
cyclopentadiene	C5H6	5	6	cyclic (diene)		cyclopentane	N/A	N/A	🟥 640	0	0	0.00%	N/A	2	2	1	0	N/A	N/A	N/A		57.748
n-hexane	C6H14	6	14	straight		hexane	N/A	N/A	🟩 227	0	0	0.00%	N/A	0	0	0	0	N/A	N/A	N/A		20.266
cis-2-hexene	C6H12	6	12	straight (diene)		hexane	N/A	N/A	🟥 252	0	0	0.00%	N/A	1	1	1	0	cis	N/A	N/A		19.832
trans-2-hexene	C6H12	6	12	straight (diene)		hexane	2	N/A	🟥 252	0	0	0.00%	N/A	1	1	1	0	trans	N/A	N/A		20.17
1-hexene	C6H12	6	12	straight (diene)		hexane	1	N/A	🟩 253	0	0	0.00%	N/A	1	1	1	0	N/A	N/A	N/A		24.054
cyclohexane	C6H12	6	12	cyclic		cyclohexane	N/A	N/A	🟥 260	0	0	0.00%	N/A	0	0	0	0	N/A	N/A	N/A		13.044
2-methylpentane	C6H14	6	14	branched (one)		pentane	N/A	2	🟩 264	1	1	16.67%	1	0	0	0	0	N/A	N/A	N/A		28.149
cyclohexene	C6H10	6	10	cyclic (diene)		cyclohexane	N/A	N/A	🟥 265	0	0	0.00%	N/A	1	1	1	0	N/A	N/A	N/A		11.918
trans-3-hexene	C6H12	6	12	straight (diene)		hexane	3	N/A	🟥 276	0	0	0.00%	N/A	1	1	1	0	trans	N/A	N/A		21.252
3-methylpentane	C6H16	6	16	branched (one)		pentane	N/A	3	🟩 278	1	1	16.67%	1	0	0	0	0	N/A	N/A	N/A		25.239
cis-3-hexene	C6H12	6	12	straight (diene)		hexane	N/A	N/A	🟥 282	0	0	0.00%	N/A	1	1	1	0	cis	N/A	N/A		21.979
2-methyl-1-pentene	C6H14	6	14	branched (one) (diene)		pentane	N/A	2	🟥 300	1	1	16.67%	1	1	1	1	0	N/A	N/A	N/A		26.079
4-methyl-1-pentene	C6H14	6	14	branched (one) (diene)		pentane	N/A	4	🟥 300	1	1	16.67%	1	1	1	1	0	N/A	N/A	N/A		36.184
3-methylenepentane	C6H12	6	12	branched (one) (diene)		pentane	N/A	N/A	🟥 315	1	2	33.33%	2	1	1	0	1	N/A	N/A	N/A		N/A
methylcyclopentane	C6H12	6	12	cyclic (substituated)		cyclopentane	N/A	N/A	🟥 329	1	1	16.67%	1	0	0	0	0	N/A	N/A	N/A		18.31
2,3-dimethyl-1-butene	C6H12	6	12	branched (two) (diene)		butane	1	N/A	🟥 360	2	2	33.33%	1	1	1	1	0	N/A	N/A	N/A		33.637
2,3-dimethylbutane	C6H14	6	14	branched (two)		butane	N/A	4	🟩 396	2	2	33.33%	1	0	0	0	0	N/A	N/A	N/A		31.311
2,3-dimethyl-2-butene	C6H12	6	12	branched (two) (diene)		butane	2	N/A	🟥 400	2	2	33.33%	1	1	1	1	0	N/A	N/A	N/A		16.663
2,2-dimethylbutane	C6H14	6	14	branched (two)		butane	N/A	5	🟩 405	2	2	33.33%	1	0	0	0	0	N/A	N/A	N/A		42.738
methylcyclopentadiene	C6H8	6	8	cyclic (substituated) (diene)		cyclopentane	N/A	N/A	🟥 446	1	1	16.67%	1	2	2	2	0	N/A	N/A	N/A		16.495
benzene	C6H6	6	6	aromatic		benzene	N/A	N/A	🟩 548	0	0	0.00%	N/A	3	0	3	0	N/A	N/A	N/A		12.69
n-heptane	C7H16	7	16	straight		heptane	N/A	N/A	🟩 213	0	0	0.00%	N/A	0	0	0	0	N/A	N/A	N/A		6.0661
methylcyclohexane	C7H14	7	14	cyclic (substituated)		cyclohexane	N/A	N/A	🟩 239	1	1	14.29%	1	0	0	0	0	N/A	N/A	N/A		6.1387
trans-2-heptene	C7H14	7	14	straight (diene)		heptane	2	N/A	🟦 258	0	0	0.00%	N/A	1	1	1	0	trans	N/A	N/A		6.1478
ethylcyclopentane	C7H14	7	14	cyclic (substituated)		cyclopentane	N/A	N/A	🟥 260	1	2	28.57%	2	0	0	0	0	N/A	N/A	N/A		5.3135
1-heptene	C7H14	7	14	straight (diene)		heptane	1	N/A	🟦 260	0	0	0.00%	N/A	1	1	1	0	N/A	N/A	N/A		7.5166
2-methylhexane	C7H16	7	16	branched (one)		hexane	N/A	2	🟥 280	1	1	14.29%	1	0	0	0	0	N/A	N/A	N/A		8.7699
trans-3-heptene	C7H14	7	14	straight (diene)		heptane	3	N/A	🟦 304	0	0	0.00%	N/A	1	1	1	0	trans	N/A	N/A		6.9794
3,3-dimethylpentane	C7H16	7	16	branched (two)		pentane	N/A	6	🟥 337	2	2	28.57%	1	0	0	0	0	N/A	N/A	N/A		11.027
2,2-dimethylpentane	C7H14	7	14	branched (two)		pentane	N/A	4	🟥 337	2	2	28.57%	1	0	0	0	0	N/A	N/A	N/A		14.039
2,4-dimentylpentane	C7H16	7	16	branched (two)		pentane	N/A	6	🟥 337	2	2	28.57%	1	0	0	0	0	N/A	N/A	N/A		N/A
2,3-dimethylpentane	C7H16	7	16	branched (two)		pentane	N/A	5	🟥 337	2	2	28.57%	1	0	0	0	0	N/A	N/A	N/A		9.1695
3-methylhexane	C7H16	7	16	branched (one)		hexane	N/A	3	🟥 450	1	1	14.29%	1	0	0	0	0	N/A	N/A	N/A		8.1865
2,2,3-trimethylbutane	C7H16	7	16	branched (three)		butane	N/A	N/A	🟩 450	3	3	42.86%	1	0	0	0	0	N/A	N/A	N/A		13.651
toluene	C7H8	7	8	aromatic (substituated)		benzene	N/A	N/A	🟦 480	1	1	14.29%	1	3	0	3	0	N/A	N/A	N/A		0.91457
2-norbornene	C7H12	7	12	cyclic (substituated)		N/A	N/A	N/A	🟥 505	2	1	14.29%	0.5	1	1	1	0	N/A	N/A	N/A		N/A (temp out of range)
n-octane	C8H18	8	18	straight		octane	N/A	N/A	🟩 206	0	0	0.00%	N/A	0	0	0	0	N/A	N/A	N/A		1.871
1-octene	C8H16	8	16	straight (diene)		octane	1	N/A	🟦 230	0	0	0.00%	N/A	1	1	1	0	N/A	N/A	N/A		2.2864
4-methylheptane	C8H18	8	18	branched (one)		heptane	N/A	4	🟦 237	1	1	12.50%	1	0	0	0	0	N/A	N/A	N/A		2.7318
ethylcyclohexane	C8H16	8	16	cyclic (substituated)		cyclohexane	N/A	N/A	🟩 238	1	2	25.00%	2	0	0	0	0	N/A	N/A	N/A		1.7249
3-methylheptane	C8H18	8	18	branched (one)		heptane	N/A	3	🟥 239	1	1	12.50%	1	0	0	0	0	N/A	N/A	N/A		2.615
2-methylheptane	C8H18	8	18	branched (one)		heptane	N/A	2	🟥 247	1	1	12.50%	1	0	0	0	0	N/A	N/A	N/A		2.7489
trans-2-octene	C8H16	8	16	straight (diene)		octane	2	N/A	🟦 250	0	0	0.00%	N/A	1	1	1	0	N/A	N/A	N/A		1.8561
n-propylcyclopentane	C8H16	8	16	cyclic (substituated)		cyclopentane	N/A	N/A	🟦 269	1	3	37.50%	3	0	0	0	0	N/A	N/A	N/A		1.6484
vinylcyclohexene	C8H10	8	10	cyclic (substituated) (diene)		cyclohexane	N/A	N/A	🟥 270	1	2	25.00%	2	2	2	1	1	N/A	N/A	N/A		1.8809
trans-3-octene	C8H16	8	16	straight (diene)		octane	3	N/A	🟦 275	0	0	0.00%	N/A	1	1	1	0	N/A	N/A	N/A		2.3053
trans-4-octene	C8H16	8	16	straight (diene)		octane	4	N/A	🟦 279	0	0	0.00%	N/A	1	1	1	0	N/A	N/A	N/A		2.3731
cis-1,2-dimethylcyclohexane	C8H16	8	16	cyclic (substituated)		cyclohexane	N/A	3	🟥 304	2	2	25.00%	1	0	0	0	0	cis	N/A	N/A		1.9305
cis-1,4-dimethylcyclohexane	C8H16	8	16	cyclic (substituated)		cyclohexane	N/A	5	🟥 304	2	2	25.00%	1	0	0	0	0	cis	N/A	N/A		2.3906
trans-1,2-dimethylcyclohexane	C8H16	8	16	cyclic (substituated)		cyclohexane	N/A	3	🟥 304	2	2	25.00%	1	0	0	0	0	trans	N/A	N/A		2.5811
1,1-dimethylcyclohexane	C8H16	8	16	cyclic (substituated)		cyclohexane	N/A	2	🟥 304	2	2	25.00%	1	0	0	0	0	N/A	N/A	N/A		3.0209
trans-1,4-dimethylcyclohexane	C8H16	8	16	cyclic (substituated)		cyclohexane	N/A	5	🟥 304	2	2	25.00%	1	0	0	0	0	trans	N/A	N/A		3.0248
trans-1,3-dimethylcyclohexane	C8H16	8	16	cyclic (substituated)		cyclohexane	N/A	4	🟥 306	2	2	25.00%	1	0	0	0	0	trans	N/A	N/A		2.3489
cis-1,3-dimethylcyclohexane	C8H16	8	16	cyclic (substituated)		cyclohexane	N/A	4	🟥 306	2	2	25.00%	1	0	0	0	0	cis	N/A	N/A		2.8632
2,4-dimethylhexane	C8H18	8	18	branched (two)		hexane	N/A	6	🟦 315	2	2	25.00%	1	0	0	0	0	N/A	N/A	N/A		4.045
2,5-dimethylhexane	C8H18	8	18	branched (two)		hexane	N/A	7	🟦 315	2	2	25.00%	1	0	0	0	0	N/A	N/A	N/A		4.0394
3,4-dimethylhexane	C8H18	8	18	branched (two)		hexane	N/A	7	🟦 315	2	2	25.00%	1	0	0	0	0	N/A	N/A	N/A		2.8877
2,3-dimethylhexane	C8H18	8	18	branched (two)		hexane	N/A	5	🟦 315	2	2	25.00%	1	0	0	0	0	N/A	N/A	N/A		3.128
2,2-dimethylhexane	C8H18	8	18	branched (two)		hexane	N/A	4	🟦 337	2	2	25.00%	1	0	0	0	0	N/A	N/A	N/A		4.5375
3,3-dimethylhexane	C8H18	8	18	branched (two)		hexane	N/A	6	🟦 337	2	2	25.00%	1	0	0	0	0	N/A	N/A	N/A		3.8136
2,4,4-trimethyl-1-pentene	C8H16	8	16	branched (three) (diene)		pentane	N/A	10	🟩 377	3	3	37.50%	1	1	1	1	0	N/A	N/A	N/A		N/A
2,2,3-trimethylpentane	C8H18	8	18	branched (three)		pentane	N/A	7	🟩 396	3	3	37.50%	1	0	0	0	0	N/A	N/A	N/A		4.2751
isooctane (2,2,4-trimethylpentane)	C8H18	8	18	branched (three)		pentane	N/A	8	🟦 411	3	3	37.50%	1	0	0	0	0	N/A	N/A	N/A		6.5762
2,3,4-trimethylpentane	C8H18	8	18	branched (three)		pentane	N/A	9	🟥 427	3	3	37.50%	1	0	0	0	0	N/A	N/A	N/A		3.6155
bicyclo[2.2.2]octane	C8H14	8	14	cyclic (polycyclic)		cyclohexane	N/A	N/A	🟦 427	0	0	0.00%	N/A	0	0	0	0	N/A	N/A	N/A		N/A (temp out of range)
2,3,3-trimethylpentane	C8H18	8	18	branched (three)		pentane	N/A	8	🟥 430	3	3	37.50%	1	0	0	0	0	N/A	N/A	N/A		3.5977
ethylbenzene	C8H10	8	10	aromatic (substituated)		benzene	N/A	N/A	🟦 431	1	2	25.00%	2	3	0	3	0	N/A	N/A	N/A		1.2795
o-xylene	C8H10	8	10	aromatic (substituated)		benzene	N/A	N/A	🟥 464	2	2	25.00%	1	3	0	0	0	N/A	ortho	N/A		0.89445
styrene	C8H8	8	8	aromatic (substituated) (diene)		benzene	N/A	N/A	🟥 490	1	2	25.00%	2	4	1	0	1	N/A	N/A	N/A		0.83092
m-xylene	C8H10	8	10	aromatic (substituated)		benzene	N/A	N/A	🟥 528	2	2	25.00%	1	3	0	0	0	N/A	meta	N/A		1.0651
p-xylene	C8H10	8	10	aromatic (substituated)		benzene	N/A	N/A	🟥 529	2	2	25.00%	1	3	0	0	0	N/A	para	N/A		1.1806
n-nonane	C9H20	9	20	straight		nonane	N/A	N/A	🟩 205	0	0	0.00%	N/A	0	0	0	0	N/A	N/A	N/A		0.58036
2-methyloctane	C9H18	9	18	branched (one)		octane	N/A	2	🟥 220	1	1	11.11%	1	0	0	0	0	N/A	N/A	N/A		0.80008
3-methyloctane	C9H18	9	18	branched (one)		octane	N/A	3	🟥 220	1	1	11.11%	1	0	0	0	0	N/A	N/A	N/A		0.83342
4-methyloctane	C9H18	9	18	branched (one)		octane	N/A	4	🟥 220	1	1	11.11%	1	0	0	0	0	N/A	N/A	N/A		0.91031
1-nonene	C9H18	9	18	straight (diene)		nonane	1	N/A	🟦 244	0	0	0.00%	N/A	1	1	1	0	N/A	N/A	N/A		0.75544
n-propylcyclohexane	C9H18	9	18	cyclic (substituated)		cyclohexane	N/A	N/A	🟦 248	1	3	33.33%	3	0	0	0	0	N/A	N/A	N/A		0.5632
trans-2-nonene	C9H18	9	18	straight (diene)		nonane	2	N/A	🟦 249	0	0	0.00%	N/A	1	1	1	0	N/A	N/A	N/A		0.65478
n-butylcyclopentane	C9H18	9	18	cyclic (substituated)		cyclopentane	N/A	N/A	🟦 250	1	4	44.44%	4	0	0	0	0	N/A	N/A	N/A		0.52893
isopropylcyclohexane	C9H18	9	18	cyclic (substituated)		cyclohexane	N/A	N/A	🟦 283	1	3	33.33%	3	0	0	0	0	N/A	N/A	N/A		0.63907
iso-butylcyclopentane	C9H18	9	18	cyclic (substituated)		cyclopentane	N/A	N/A	🟦 288	1	4	44.44%	4	0	0	0	0	N/A	N/A	N/A		0.85491
1,1,3-trimethylcyclohexane	C9H18	9	18	cyclic (substituated)		cyclohexane	N/A	5	🟦 310	3	3	33.33%	1	0	0	0	0	N/A	N/A	N/A		1.489
1-trans-3,5-trimethylcyclohexane	C9H18	9	18	cyclic (substituated)		cyclohexane	N/A	N/A	🟦 314	3	3	33.33%	1	0	0	0	0	trans	N/A	N/A		1.552
2,4-dimethyl-3-ethylpentane	C9H20	9	20	branched (three)		pentane	N/A	9	🟥 390	3	4	44.44%	1.333333333	0	0	0	0	N/A	N/A	N/A		1.3359
cumene (2-phenylpropane)	C9H12	9	12	aromatic (substituated)		benzene	N/A	N/A	🟥 424	1	3	33.33%	3	3	0	0	0	N/A	N/A	N/A		0.60861
2,2,3,3-tetramethylpentane	C9H20	9	20	branched (four)		pentane	N/A	10	🟥 430	4	4	44.44%	1	0	0	0	0	N/A	N/A	N/A		1.2683
2,2,3,4-tetramethylpentane	C9H20	9	20	branched (four)		pentane	N/A	11	🟥 430	4	4	44.44%	1	0	0	0	0	N/A	N/A	N/A		1.6902
2,2,4,4-tetramethylpentane	C9H20	9	20	branched (four)		pentane	N/A	12	🟥 430	4	4	44.44%	1	0	0	0	0	N/A	N/A	N/A		2.6713
o-ethyltoluene	C9H12	9	12	aromatic (substituated)		benzene	N/A	N/A	🟥 440	2	3	33.33%	1.5	3	0	0	0	N/A	ortho	N/A		0.33911
n-propylbenzene	C9H14	9	14	aromatic (substituated)		benzene	N/A	N/A	🟥 456	1	3	33.33%	3	3	0	0	0	N/A	N/A	N/A		0.4639
1,2,3-trimethylbenzene	C9H12	9	12	aromatic (substituated)		benzene	N/A	6	🟥 470	3	3	33.33%	1	3	0	0	0	N/A	N/A	N/A		0.21646
p-ethyltoluene	C9H12	9	12	aromatic (substituated)		benzene	N/A	N/A	🟥 475	2	3	33.33%	1.5	3	0	0	0	N/A	para	N/A		0.39803
m-ethyltoluene	C9H12	9	12	aromatic (substituated)		benzene	N/A	N/A	🟥 480	2	3	33.33%	1.5	3	0	0	0	N/A	meta	N/A		0.42429
m-methylstyrene	C9H10	9	10	aromatic (substituated) (diene)		benzene	N/A	N/A	🟥 489	2	3	33.33%	1.5	4	1	0	1	N/A	meta	N/A		0.25304
1,2,4-trimethylbenzene	C9H12	9	12	aromatic (substituated)		benzene	N/A	7	🟥 515	3	3	33.33%	1	3	0	0	0	N/A	N/A	N/A		0.2868
mesitylene	C9H12	9	12	aromatic (substituated)		benzene	N/A	N/A	🟥 550	3	3	33.33%	1	3	0	0	0	N/A	N/A	N/A		0.33688
p-methylstyrene	C9H10	9	10	aromatic (substituated) (diene)		benzene	N/A	N/A	🟥 575	2	3	33.33%	1.5	4	1	0	1	N/A	para	N/A		0.24364
n-decane	C10H22	10	22	straight		decane	N/A	N/A	🟩 201	0	0	0.00%	N/A	0	0	0	0	N/A	N/A	N/A		0.181
3-methylnonane	C10H22	10	22	branched (one)		nonane	N/A	3	🟦 212	1	1	10.00%	1	0	0	0	0	N/A	N/A	N/A		0.26373
5-methylnonane	C10H22	10	22	branched (one)		nonane	N/A	5	🟦 212	1	1	10.00%	1	0	0	0	0	N/A	N/A	N/A		0.29402
4-methylnonane	C10H22	10	22	branched (one)		nonane	N/A	4	🟦 212	1	1	10.00%	1	0	0	0	0	N/A	N/A	N/A		0.30874
2-methylnonane	C10H22	10	22	branched (one)		nonane	N/A	2	🟦 214	1	1	10.00%	1	0	0	0	0	N/A	N/A	N/A		0.25128
1-decene	C10H20	10	20	straight (diene)		decane	1	N/A	🟥 235	0	0	0.00%	N/A	1	1	1	0	N/A	N/A	N/A		0.24325
n-pentylcyclopentane	C10H20	10	20	cyclic (substituated)		cyclopentane	N/A	N/A	🟦 239	1	5	50.00%	5	0	0	0	0	N/A	N/A	N/A		0.15817
trans-2-decene	C10H20	10	20	straight (diene)		decane	2	N/A	🟦 242	0	0	0.00%		1	1	1	0	trans	N/A	N/A		0.18398
n-butylcyclohexane	C10H20	10	20	cyclic (substituated)		cyclohexane	N/A	N/A	🟥 246	1	4	40.00%	4	0	0	0	0	N/A	N/A	n		0.17606
cis-decahydronaphthalene (cis-decalin)	C10H18	10	18	cyclic (polycyclic)		cyclohexane	N/A	N/A	🟥 250	0	0	0.00%	N/A	0	0	0	0	cis	N/A	N/A		0.10457
trans-decahydronapthalene (trans-decalin)	C10H18	10	18	cyclic (polycyclic)		cyclohexane	N/A	N/A	🟥 250	0	0	0.00%	N/A	0	0	0	0	trans	N/A	N/A		0.1653
iso-butylcyclohexane	C10H20	10	20	cyclic (substituated)		cyclohexane	N/A	N/A	🟦 274	1	4	40.00%	4	0	0	0	0	N/A	N/A	iso		0.28683
sec-butylcyclohexane	C10H20	10	20	cyclic (substituated)		cyclohexane	N/A	N/A	🟦 277	1	4	40.00%	4	0	0	0	0	N/A	N/A	sec		0.20378
tert-butylcyclohexane	C10H20	10	20	cyclic (substituated)		cyclohexane	N/A	N/A	🟦 342	1	4	40.00%	4	0	0	0	0	N/A	N/A	tert		0.31046
1,2,3,4-tetramethylcyclohexane	C10H20	10	20	cyclic (substituated)		cyclohexane	N/A	N/A	🟦 370	4	4	40.00%	1	0	0	0	0	N/A	N/A	N/A		0.19257
o-cymene	C10H14	10	14	aromatic (substituated)		benzene	N/A	N/A	🟥 377	2	4	40.00%	2	3	0	0	0	N/A	ortho	N/A		0.21954
1,2,3,4-tetrahydronapthalene	C10H12	10	12	aromatic (substituated)		N/A	N/A	N/A	🟥 384	1	4	40.00%	4	3	0	0	0	N/A	N/A	N/A		0.049538
o-diethylbenzene	C10H14	10	14	aromatic (substituated)		benzene	N/A	N/A	🟥 395	2	4	40.00%	2	3	0	0	0	N/A	ortho	N/A		0.14049
1-methylindan	C10H12	10	12	aromatic (polycyclic)		N/A	N/A	N/A	🟦 412	1	1	10.00%	1	3	0	0	0	N/A	N/A	N/A		0.13267
n-butylbenzene	C10H14	10	14	aromatic (substituated)		benzene	N/A	N/A	🟥 412	1	4	40.00%	4	3	0	0	0	N/A	N/A	n		0.14326
sec-butylbenzene	C10H14	10	14	aromatic (substituated)		benzene	N/A	N/A	🟥 418	1	4	40.00%	4	3	0	0	0	N/A	N/A	sec		0.22407
prehnitene (1,2,3,4-tetramethylbenzene)	C10H14	10	14	aromatic (substituated)		benzene	N/A	N/A	🟦 427	4	4	40.00%	1	3	0	0	0	N/A	N/A	N/A		0.044195
isodurene (1,2,3,5-tetramethylbenzene)	C10H14	10	14	aromatic (substituated)		benzene	N/A	N/A	🟦 427	4	4	40.00%	1	3	0	0	0	N/A	N/A	N/A		0.06639
durene (1,2,4,5-tetramethylbenzene)	C10H14	10	14	aromatic (substituated)		benzene	N/A	N/A	🟦 427	4	4	40.00%	1	3	0	0	0	N/A	N/A	N/A		N/A (out of range)
iso-butylbenzene	C10H14	10	14	aromatic (substituated)		benzene	N/A	N/A	🟦 428	1	4	40.00%	4	3	0	0	0	N/A	N/A	iso		0.26479
p-diethylbenzene	C10H14	10	14	aromatic (substituated)		benzene	N/A	N/A	🟥 430	2	4	40.00%	2	3	0	0	0	N/A	para	N/A		0.13685
p-cymene	C10H14	10	14	aromatic (substituated)		benzene	N/A	N/A	🟥 436	2	4	40.00%	2	3	0	0	0	N/A	para	N/A		0.1994
m-cymene	C10H14	10	14	aromatic (substituated)		benzene	N/A	N/A	🟥 436	2	4	40.00%	2	3	0	0	0	N/A	meta	N/A		0.23218
m-diethylbenzene	C10H14	10	14	aromatic (substituated)		benzene	N/A	N/A	🟥 450	2	4	40.00%	2	3	0	0	0	N/A	meta	N/A		0.16037
tert-butylbenzene	C10H14	10	14	aromatic (substituated)		benzene	N/A	N/A	🟥 450	1	4	40.00%	4	3	0	0	0	N/A	N/A	tert		0.29068
dicyclopentadiene	C10H12	10	12	polycyclic (substituated) (diene)		cyclopentane	N/A	N/A	🟥 510	1	1	10.00%	1	2	2	0	0	N/A	N/A	N/A		N/A (temp out of range)
naphthalene	C10H8	10	8	aromatic (polycyclic)		naphthalene	N/A	N/A	🟥 587	0	0	0.00%	N/A	5	0	0	0	N/A	N/A	N/A		N/A (temp out of range)
n-undecane	C11H24	11	24	straight		undecane	N/A	N/A	🟥 202	0	0	0.00%	N/A	0	0	0	0	N/A	N/A	N/A		0.055622
3-methyldecane	C11H24	11	24	straight (substituated)		decane	N/A	3	🟦 210	1	1	9.09%	1	0	0	0	0	N/A	N/A	N/A		0.091951
2-methyldecane	C11H24	11	24	branched (one)		decane	N/A	2	🟦 229	1	1	9.09%	1	0	0	0	0	N/A	N/A	N/A		0.079922
1-undecene	C11H22	11	22	straight (diene)		undecane	1	N/A	🟥 237	0	0	0.00%	N/A	1	1	1	0	N/A	N/A	N/A		0.079009
n-pentylcyclohexane	C11H22	11	22	cyclic (substituated)		cyclohexane	N/A	N/A	🟦 244	1	5	45.45%	5	0	0	0	0	N/A	N/A	N/A		0.057429
1-methyldecalin	C11H20	11	20	cyclic (polycyclic) (substituated)		cyclohexane	N/A	N/A	🟦 263	1	1	9.09%	1	0	0	0	0	N/A	N/A	N/A		0.030262
p-isopropylphenylstyrene	C11H12	11	12	aromatic (substituated)		benzene	N/A	N/A	🟦 339	2	5	45.45%	2.5	5	2	0	2	N/A	N/A	N/A		N/A (temp out of range)
pentamethylbenzene	C11H16	11	16	aromatic (substituated)		benzene	N/A	N/A	🟦 430	5	5	45.45%	1	3	0	0	0	N/A	N/A	N/A		N/A (temp out of range)
1-methylnaphthalene	C11H10	11	10	aromatic (polycyclic) (substituated)		naphthalene	N/A	N/A	🟥 529	1	1	9.09%	1	5	0	0	0	N/A	N/A	N/A		0.010038
2-methylnaphthalene	C11H10	11	10	aromatic (polycyclic) (substituated)		naphthalene	N/A	N/A	🟥 529	1	1	9.09%	1	5	0	0	0	N/A	N/A	N/A		N/A (temp out of range)
n-dodecane	C12H26	12	26	straight		dodecane	N/A	N/A	🟥 200	0	0	0.00%	N/A	0	0	0	0	N/A	N/A	N/A		0.017868
3-methylundecane	C12H26	12	26	branched (one)		undecane	N/A	3	🟦 210	1	1	8.33%	1	0	0	0	0	N/A	N/A	N/A		0.33363
2-methylundecane	C12H26	12	26	branched (one)		undecane	N/A	2	🟦 224	1	1	8.33%	1	0	0	0	0	N/A	N/A	N/A		0.027291
trans-2-dodecene	C12H24	12	24	straight (diene)		dodecane	2	N/A	🟦 240	0	0	0.00%	N/A	1	1	1	0	trans	N/A	N/A		0.016606
n-hexylcyclohexane	C12H24	12	24	cyclic (substituated)		cyclohexane	N/A	N/A	🟦 241	1	6	50.00%	6	0	0	0	0	N/A	N/A	N/A		0.017365
bicyclohexyl	C12H22	12	22	cyclic (polycyclic)		cyclohexane	N/A	N/A	🟥 245	0	0	0.00%	N/A	0	0	0	0	N/A	N/A	N/A		0.014331
1-dodecene	C12H24	12	24	straight (diene)		dodecane	1	N/A	🟦 255	0	0	0.00%	N/A	1	1	1	0	N/A	N/A	N/A		0.024429
1-tert-butyl-4-ethylbenzene	C12H18	12	18	aromatic (substituated)		benzene	N/A	N/A	🟦 280	2	6	50.00%	3	3	0	0	0	N/A	para	tert		0.036479
cyclohexylbenzene	C12H16	12	16	aromatic (substituated)		benzene	N/A	N/A	🟦 294	1	6	50.00%	6	3	0	0	0	N/A	N/A	N/A		0.010752
p-diisopropylbenzene	C12H18	12	18	aromatic (substituated)		benzene	N/A	N/A	🟥 413	2	6	50.00%	3	3	0	0	0	N/A	para	N/A		0.034553
m-diisopropylbenzene	C12H18	12	18	aromatic (substituated)		benzene	N/A	N/A	🟥 413	2	6	50.00%	3	3	0	0	0	N/A	meta	N/A		0.04654
1-ethylnaphthalene	C12H12	12	12	aromatic (polycyclic) (substituated)		naphthalene	N/A	N/A	🟥 480	1	2	16.67%	2	5	0	0	0	N/A	N/A	N/A		0.0033207
diphenyl	C12H10	12	10	aromatic (polycyclic)		benzene	N/A	N/A	🟦 540	0	0	0.00%	N/A	6	0	0	0	N/A	N/A	N/A		N/A (temp out of range)
n-tridecane	C13H28	13	28	straight		tridecane	N/A	N/A	🟥 202	0	0	0.00%	N/A	0	0	0	0	N/A	N/A	N/A		0.0056899
3-methyldodecane	C13H28	13	28	branched (one)		dodecane	N/A	3	🟦 210	1	1	7.69%	1	0	0	0	0	N/A	N/A	N/A		0.011518
2-methyldodecane	C13H28	13	28	branched (one)		dodecane	N/A	2	🟦 221	1	1	7.69%	1	0	0	0	0	N/A	N/A	N/A		0.010014
1-tridecene	C13H26	13	26	straight (diene)		tridecane	1	N/A	🟥 237	0	0	0.00%	N/A	1	1	1	0	N/A	N/A	N/A		0.0080727
n-heptylbenzene	C13H20	13	20	aromatic (substituated)		benzene	N/A	N/A	🟦 324	1	7	53.85%	7	3	0	0	0	N/A	N/A	N/A		0.0050003
1-n-propylnaphthalene	C13H14	13	14	aromatic (polycyclic) (substituated)		naphthalene	N/A	N/A	🟦 417	1	3	23.08%	3	5	0	0	0	N/A	N/A	N/A		0.00176
diphenylmethane	C13H12	13	12	aromatic (polycyclic) (substituated)		N/A	N/A	N/A	🟥 485	1	1	7.69%	1	6	0	0	0	N/A	N/A	N/A		0.0019936
n-tetradecane	C14H30	14	30	straight		tetradecane	N/A	N/A	🟥 200	0	0	0.00%	N/A	0	0	0	0	N/A	N/A	N/A		0.0018642
3-methyltridecane	C14H30	14	30	branched (one)		tridecane	N/A	3	🟦 210	1	1	7.14%	1	0	0	0	0	N/A	N/A	N/A		0.0031507
2-methyltridecane	C14H30	14	30	branched (one)		tridecane	N/A	2	🟦 219	1	1	7.14%	1	0	0	0	0	N/A	N/A	N/A		0.0033872
1-tetradecene	C14H28	14	28	straight (diene)		tetradecane	1	N/A	🟥 235	0	0	0.00%	N/A	1	1	1	0	N/A	N/A	N/A		0.0023594

🟩 FROM AFFENS PAPER
🟥 from chemical properties handbook (Laws)
🟦 from DIPPR database

1,2,3,5-tetraethylbenzene	C14H22	14	22	aromatic (substituated)		benzene	N/A	11	325	4	8	57.14%	2	3	0	0	0	N/A	N/A	N/A		0.0018098
1-n-butylnaphthalene	C14H16	14	16	aromatic (polycyclic) (substituated)		naphthalene	N/A	N/A	360	1	4	28.57%	4	5	0	0	0	N/A	N/A	N/A		0.0004378
1,1-diphenylethane	C14H14	14	14	aromatic (polycyclic) (substituated)		benzene	N/A	N/A	440	1	2	14.29%	2	6	0	0	0	N/A	N/A	N/A		0.0015531
1,2-diphenylethane	C14H14	14	14	aromatic (polycyclic) (substituated)		benzene	N/A	N/A	480	1	2	14.29%	2	6	0	0	0	N/A	N/A	N/A		N/A (temp out of range)
phenanthrene	C14H10	14	10	aromatic (polycyclic)		N/A	N/A	N/A	540	0	0	0.00%	N/A	7	0	0	0	N/A	N/A	N/A		N/A (temp out of range)
anthracene	C14H10	14	10	aromatic (polycyclic)		N/A	N/A	N/A	540	0	0	0.00%	N/A	7	0	0	0	N/A	N/A	N/A		N/A (temp wayyy too low)
n-pentadecane	C15H32	15	32	straight		pentadecane	N/A	N/A	202	0	0	0.00%	N/A	0	0	0	0	N/A	N/A	N/A		0.00065487
1-pentadecene	C15H30	15	30	straight (diene)		pentadecane	1	N/A	237	0	0	0.00%	N/A	1	1	1	0	N/A	N/A	N/A		0.00077909
trans-2-pentadecene	C15H30	15	30	straight (diene)		pentadecane	2	N/A	238	0	0	0.00%	N/A	1	1	1	0	trans	N/A	N/A		0.0011792
1-n-pentylnaphthalene	C15H18	15	18	aromatic (polycyclic) (substituated)		naphthalene	N/A		307	1	5	33.33%	5	3	0	0	0	N/A	N/A	N/A		0.00016058
1,3,5-triisopropylbenzene	C15H24	15	24	aromatic (substituated)		benzene	N/A	9	350	3	9	60.00%	3	3	0	0	0	N/A	N/A	N/A		0.0054588
4-methylphenanthrene	C15H12	15	12	aromatic (polycyclic) (substituated)		N/A	N/A		523	1	1	6.67%	1	7	0	0	0	N/A	N/A	N/A		N/A (temp out of range)
n-hexadecane	C16H34	16	34	straight		hexadecane	N/A	N/A	201	0	0	0.00%	N/A	0	0	0	0	N/A	N/A	N/A		0.00017441
pentaethylbenzene	C16H26	16	26	aromatic (substituated)		benzene	N/A	N/A	293	5	10	62.50%	2	3	0	0	0	N/A	N/A	N/A		0.0002879
2,2,4,4,6,8,8-heptamethylnonane (isocetane)	C16H34	16	34	branched (seven)		nonane	N/A	34	705	7	7	43.75%	1	0	0	0	0	N/A	N/A	N/A		0.0064232
n-heptadecane	C17H36	17	36	straight		heptadecane	N/A	N/A	202	0	0	0.00%	N/A	0	0	0	0	N/A	N/A	N/A		0.000057416
1-heptadecene	C17H34	17	34	straight (diene)		heptadecane	1	N/A	230	0	0	0.00%	N/A	1	1	1	0	N/A	N/A	N/A		0.000069241